A129837

CRACK ARREST TOUGHNESS OF 4140 [illegible] AND 4340 STEEL

U. S. ARMAMENT Research and Development Command

Contract No. DAAK-10-80-C-9257

[illegible]

by

E. J. [illegible] and P. B. Crosley

November 1981

Materials Research Laboratory, Inc.

One Science Road
Glenwood, Illinois 60425

♦ Area Code 312
♦ Locai telephone 755-8760
♦ Chicago telephone 785-4020

CRACK ARREST TOUGHNESS OF 4140, 1340 AND 4340 STEEL

For
U. S. Armament Research and Development Command
Contract No. DAAK-10-80-C-0287
(MRL No. 792)

By
E. J. Ripling and P. B. Crosley

November 1981

Materials
Research
Laboratory,
Inc.

One Science Road
Glenwood, Illinois 60425

- Area Code 312
- Local telephone 755-8760
- Chicago telephone 785-4020

CRACK ARREST TOUGHNESS OF 4140, 1340 AND 4340 STEEL

For

U. S. Army Armament Research and Development Command

Contract No. DAAK-10-80-C-0287

(MRL No. 792)

By

E. J. Ripling and P. B. Crosley

November 1981

Materials
Research
Laboratory
Inc

CRACK ARREST TOUGHNESS OF 4140, 1340 AND 4340 STEEL

For

U. S. Army Armament Research and Development Command
Contract No. DA[illegible]-10-80-C-0287
(MRL No. 792)

By

E. J. Ripling and P. B. Crosley

November 1981

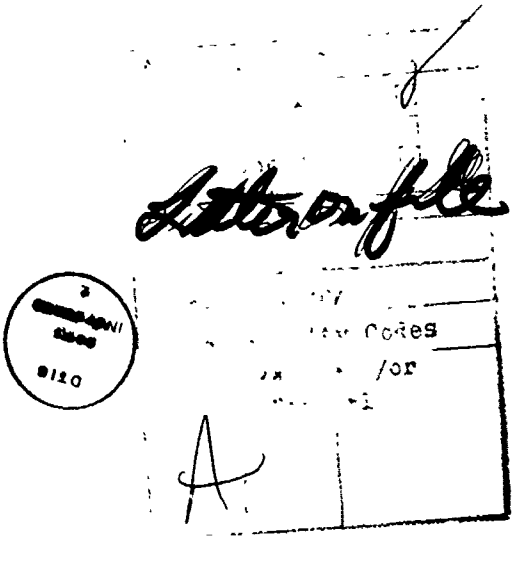

1.0 Introduction

Armament materials are generally used in structures that are rapidly loaded, and, of course, this service condition must be considered when evaluating their fracture properties. Collecting initiation toughness data at very high loading rates is difficult, however, because of test machine and load cell vibration. These problems can be avoided by measuring crack arrest toughness, K_a, rather than rapid initiation toughness, because K_a is thought to represent the lower limit of toughness that is obtained with continuously increasing loading rates.

In an earlier study, the crack arrest fracture toughness of 4140 and 4340 steel was measured as a function of yield strength and test temperature[1]. The yield strength was varied over the range of 140 to 180 ksi, and the temperature from -65 to +165F, the ranges of most interest for armament materials. Both materials were evaluated with full-thick specimens using one-inch thick plates. In this thickness, 4340 through hardens, while 4140 does not, so that the toughness difference reported for these two materials was a result of both composition and microstructure differences. The present study was undertaken to add 1340 steel to the comparison. However, to avoid having mixed microstructures, the 1340 and two new heats of 4140 steel were heat treated in thinner sections so that they would be martensitic through their thickness.

2.0 Materials and Heat Treatment

Two plates of 4140 were purchased, one 3/4 inch, and the other $\frac{1}{2}$ inch, thick. A plate of $\frac{1}{2}$ inch thick 1340 was also supplied by the Bethlehem Steel Company.

All plates were heat treated in 6 inch by 6 inch blanks as follows: Normalize 1600°F, 1 hr; Austenitize 1550°F, 1 hr; oil quench

150-175°F; and temper 4140 at 800°F and 1340 at 400°F, 1 hr. Specimen blanks were then retempered as needed to obtain the required yield strengths.

3.0 Material Characterization

3.1 Chemical Composition and Microstructure

The chemical composition of the plates is shown in Table 1, and their microstructures in Fig. 1. Unlike the case for the one inch thick 4140 used in the earlier study, these heat treated blanks had a uniform microstructure (and hardness) through the thickness.

3.2 Tensile Properties

In order to determine the tempering temperatures to be used for obtaining the required values of yield strength, tensile specimen blanks of the 4140 steel blanks were tempered at temperatures between 800 and 1100°F, and the 1340 steel blanks at temperatures between 700 amd 1100°F. Tensile specimens (0.357 inch dia., in the TL orientation) were machined from the blanks and tested at room temperature. These results are shown in Figs. 2, 3 and 4, and Tables 2 and 3. The data show that for yield strengths of 140, 160 and 180 ksi, respectively, the 4140 should be tempered at 950, 1000 and 1100°F, and the 1340 at 750, 825 and 925°F.

Because toughness tests were to be run at -65 and 165°F, as well as room temperature, tensile tests were run at these temperatures as well, Tables 4 and 5 and Figs. 5 to 8.

4.0 Crack Arrest Fracture Toughness Tests

In the earlier study on 4140 and 4340, specimens having three different in-plane dimensions were used. Since this demor strated the specimen insensitivity of the test, only one specimen shape was used in the present study for both the ½ and 3/4 inch thick specimens. The specimen dimensions are shown in Fig. 9. The knife-edge had to be modified from that used in ASTM Standard E399 so that the arms of the

displacement gage would be trapped. The modified knife edges are also shown in Fig. 9.

All of the toughness data collected on ' rogram are shown in Tables 6 and 7.

4.1 Toughness vs. Test Temperature

The crack arrest toughness of 4140 in both thicknesses, and 1340 in ½ inch thickness is shown in Figs. 10 and 11 with yield strength as the parameter. The 4340 data collected on one inch thick specimens in the earlier study are also plotted in this same fashion in Fig. 12. If the data in these three charts are to be compared, it is necessary to know whether or not they are all plane-strain values. In the present proposed ASTM Standard on Crack Arrest Fracture Toughness Testing, the size requirement for plane strain cracking is:

$$B \geq 1.25 [K_a/(\sigma_{ys} + \sigma_o)]^2$$

where

B = critical specimen dimensions (in this case thickness)
σ_{ys} = yield strength
σ_o = 30 ksi

Hence for 140 ksi yield strength steel tested at 165°F, at which temperature its yield strength ≃ 130 ksi, the maximum value of K_a that can be measured for ½, 3/4 and one inch specimens are 101, 124 and 143 ksi-in$^{\frac{1}{2}}$, respectively. This would suggest that all the data shown in Figs. 10 to 12 are plane strain with the exception of the ½ inch thick, 140 yield strength data on 4140. Even for this material, the ½ and 3/4 inch data overlap so that all data will be treated as plane-strain values throughout this report.*

---

* It might be mentioned that a few ½ inch thick CCA specimen tests were made on 4140 in the earlier study, and in general K_a was higher for the ½ inch thick than the one inch thick specimens. The reason for this is not apparent at this time.

The most pronounced feature of these data is the well defined toughness peak that separates the transition and super-transition temperatures for 4140 steel. The occurrence of a transition temperature for both 4140 and 4340 had been reported previously; however, the pronounced peak that requires a decrease in toughness with increasing temperature was not found in the early program.

The fracture surfaces of the 4140 specimens were examined in a scanning electron microscope, and as shown on the 160 yield strength chart of Fig. 10, at the highest sub-transition temperature the fracture was primarily cleavage and at the lowest super-transition temperature, it was primarily dimpled rupture. These fracture surfaces are shown in Fig. 13. There is little question that the transition temperature is a result of a change in fracture mechanism.

The toughness of 1340 is far less dependent on test temperature than either 4140 or 4340. (Compare Fig. 11 with Figs. 10 and 12.) This is a result of the fact that even at super-transition temperatures, the toughness is moderate, e.g., all the 160 ksi yield strength specimens showed primarily dimpled rupture in spite of the fact that K_a was only about 50 ksi-in$^{\frac{1}{2}}$. At the highest yield strength, where there was a significant effect of test temperature on K_a, the fracture appearance did change from mainly cleavage to almost all dimpled rupture, as indicated in Fig. 11, and shown by the photographs in Fig. 14.

4.2 Toughness Comparisons

The toughness of the three steels are compared in Figs. 15, 16 and 17, as a function of yield strength with test temperature as the parameter. For all test temperatures and strength levels, the 4340 is markedly tougher than the other two. The 4140 is also tougher than the 1340, and at yield strengths of 140 and 160 ksi, the difference in the two steels is large. However, as the strength is increased to 180 ksi, this difference becomes less pronounced, and on testing at 165 and -65°F, the toughness of the two steels overlaps.

5.0 Effect of Side Grooves

In making crack arrest toughness tests, side grooves are added to the specimen to insure that the crack front is straight at the time of arrest. This is important for two reasons: (1) only straight cracks can be analyzed by presently available two-dimensional stress analyses, and (2) if the crack front shape changes as the crack extends, then K_a will be a function of Δa, as is the case with K_c.

The need for a straight crack front to allow for a two-dimensional analysis of the specimen could be avoided, of course, by defining crack lengths in terms of an "effective length", and this can be done by the use of a compliance technique. Because this is an important first step in developing an arrest test without side grooves, preliminary tests of this nature have been conducted and are described in the Appendix.

The manner in which the crack front shape changes with crack extension is a far more complex problem. The run-arrest event in K_a testing is usually started with a straight machined notch. Hence, the full crack front experiences the same value of K, and since the stress state is essentially constant over the width of the notch plane, the crack propagates with a reasonably straight front. In the absence of side grooves, the edges of the crack front near the specimen surface can experience no greater constraint than plane stress. Hence, the crack tends to tunnel. The amount of tunneling will depend on the material thickness, and the difference between the metal's plane stress and plane strain toughness, which, in turn, is expected to be a function of both the type of material and test temperature.

When a crack tunnels, the surface uncracked ligaments act as closing forces on the expanding crack so that the presence of side grooves should be expected to lead to conservative values of K_a. The level of conservatism is expected to depend on the type of crack that occurs in the structure that the specimen is modeling. For example, if part-through cracks are expected, then K_a with side grooves is not at all conservative, if long-running through cracks are expected, the specimen data may be unrealistically conservative. In order to measure

this level of conservatism, K_a tests without side grooves were run to compare with K_a values measured with side grooved CCA tests. Two types of specimens were used: TDCB and CCA.

5.1 Comparative Tests

The TDCB specimen is ideally suited for making crack arrest tests in the absence of side grooves because the problem of determining the crack length at arrest is avoided. Hence, room temperature tests were run, as a function of yield strength on $\frac{1}{2}$ inch thick 4140 plates using the specimen whose dimensions are shown in Fig. 18. It is important to note that the machined starter notch in this test series had a 0.002 inch radius. Single tests were run on specimens having yield strengths of 140, 160 and 180 ksi. These results are compared with CCA specimen tests with side grooves in the top chart of Fig. 19. It is obvious that the TDCB specimens without side grooves, but sharp starter notches, and the CCA specimens with side grooves produced almost identical results.

Testing the TDCB specimens at room temperature with sharp notch starters encouraged small crack jumps. A second series of tests was also run in which an attempt was made to encourage larger crack jumps. Unside-grooved CCA specimens were used for this series (although the test results are expected to be independent of specimen type). These specimens used a 0.010 inch starter notch radius, however, and were tested at -65°F. The lower test temperature in conjunction with the more blunt starter notch, did, indeed, encourage larger crack jumps, but essentially all the crack extension occurred by tunneling. The plane stress surface material essentially remained pinned so that formally calculated K_a values were quite high, even if the center-plane crack length was used, as shown in the bottom chart of Fig. 19.

To be certain that the different behaviors shown by the top and bottom charts in Fig. 19 were not the result of using TDCB vs.

CCA specimens, one CCA specimen with an 0.002 inch radius crack starter was tested at room temperature. As shown in Fig. 19 top, K_c obtained on this specimen was the same as that obtained on the TDCB specimens.

Hence, it must be concluded, at least on the basis of this limited amount of data, that for short crack jumps, the presence or absence of side grooves does not significantly change K_a. For long running cracks, on the other hand, K_a data collected on side-grooved specimens is conservative.

6.0 Conclusions

The plane strain crack arrest fracture toughness of 4140 and 1340, both in a fully Martensite condition, were measured over a yield strength range of 240 to 180 ksi, and a test temperature range of -65 to 165°F. These results were compared with each other and with the data collected earlier on 4340. The 4340 was found to be far tougher than the other two alloys at all yield strengths and test temperatures. The 4140 was tougher than the 1340, but the difference was less as the yield strength increased.

Table 1

CHEMICAL COMPOSITION OF TEST PLATES

Plate	C	Mn	Si	P	S	Cr	Mo
3/4 inch 4140 (B plate)	0.43	0.89	0.29	0.008	0.016	0.96	0.24
½ inch 4140 (C plate)	0.41	0.86	0.27	0.010	0.014	0.91	0.24
Limits for AISI-SAE (from ASM Handbook, Vol. 1)	0.38 0.43	0.75 1.00	0.15 0.30	0.035 max	0.040 max	0.80 1.10	0.15 0.25
½ inch 1340 (D plate)	0.42	1.65	0.21	0.017	0.022		
Limits for AISI-SAE (from ASM Handbook, Vol. 1	0.38 0.43	1.60 1.90	0.15 0.30	0.035 max	0.040 max		

Table 2

TENSILE PROPERTIES OF 4140 STEEL AT ROOM TEMPERATURE
(0.357 inch dia. specimens, TL orientation)

Tempering Temp. (°F)	Specimen No.	Tensile Strength (ksi)	Yield Strength (ksi)	% e	% RA
½ inch thick					
1100	C-13	149.8	136.3	14.3	41.7
1100	C-14	149.3	137.4	15.4	43.1
1050	C-11	161.8	151.2	12.9	39.4
1050	C-12	163.7	152.9	12.9	39.1
800	C-9	224.4	209.9	7.9	27.3
800	C-10	224.7	209.6	7.5	27.6
1000	C-21	170.6	160.4	12.1	39.5
1000	C-22	170.1	160.5	12.1	38.6
900	C-3	196.1	185.0	10.4	35.2
900	C-4	196.6	185.2	9.6	33.4
800	C-1	226.2	211.2	7.5	28.8
800	C-2	224.3	208.8	6.4	24.9
3/4 inch thick					
1100	B-13	153.4	138.7	13.0	40.0
1100	B-14	153.4	138.7	13.0	40.0
1050	B-11	169.1	156.0	11.0	36.1
1050	B-12	168.6	155.4	11.0	37.2
800	B-9	231.6	216.7	6.5	23.5
800	B-10	230.8	214.4	6.0	21.5
1000	B-21	177.1	165.3	10.5	35.2
1000	B-22	177.4	162.8	10.5	33.9
900	B-3	202.7	189.3	9.0	30.9
900	B-4	203.9	190.7	8.5	30.5
800	B-1	228.8	211.3	7.5	25.1
800	B-2	228.8	210.3	7.5	25.6

Materials Research Laboratory Inc

Table 3

TENSILE PROPERTIES OF 1340 STEEL AT ROOM TEMPERATURE
(0.357 inch dia. specimens, TL orientation)

Tempering Temp. (°F)	Specimen No.	Tensile Strength (ksi)	Yield Strength (ksi)	% e	% RA
1100	D-15	127.5	113.0	16.8	41.2
1100	D-16	127.6	112.2	16.8	40.7
1050	D-13	134.6	119.7	14.6	38.8
1050	D-14	135.0	121.0	15.7	40.0
1000	D-9	142.3	128.7	14.3	37.5
1000	D-10	142.1	128.2	13.9	39.2
950	D-7	146.8	133.4	12.1	38.0
950	D-8	148.5	134.0	12.5	36.6
900	D-5	160.0	146.6	11.8	35.5
900	D-6	158.0	146.5	10.4	34.3
800	D-3	176.5	165.4	9.6	31.6
800	D-4	176.1	164.4	9.6	31.6
750	D-23	199.6	185.5	7.9	28.3
750	D-24	200.2	185.2	7.5	24.0
700	D-25	214.0	196.2	7.1	23.6
700	D-26	212.9	193.7	7.1	24.0

Table 4

TENSILE PROPERTIES OF 1340 STEEL AT -65 AND +165F
(0.357 inch dia. specimens, TL orientation)

Tempering Temp. (°F)	Specimen No.	Tensile Strength (ksi)	Yield Strength (ksi)	% e	% RA
-65°F Testing Temperature					
925	D-19	166.8	151.1	11.8	31.6
925	D-20	166.8	151.0	13.2	35.3
825	D-17	184.8	169.2	10.7	28.8
825	D-18	184.4	169.7	10.7	32.1
750	D-27	207.5	191.5	8.9	28.8
750	D-28	207.9	191.4	9.6	27.1
+165°D Testing Temperature					
925	D-41	145.1	131.0	16.1	55.6
925	D-42	145.5	132.9	16.8	57.4
825	D-39	169.0	151.6	12.9	47.0
825	D-40	164.8	148.2	15.4	57.5
750	D-29	187.0	168.4	7.9	25.9
750	D-30	189.4	168.4	7.9	27.3

Table 5

TENSILE PROPERTIES OF 4140 STEEL AT -65 AND +165°F
(0.357 inch dia. specimens, TL orientation)

Tempering Temp. (°F)	Spec. No.	Tensile Strength (ksi)	Yield Strength (ksi)	% e	% RA
-65°F Testing Temperatures					
1100	C 69	159.3	146.6	15.7	42.0
1100	C 70	159.6	144.3	16.1	40.6
1000	C 66	178.4	168.6	14.3	37.2
1000	C 67	178.8	168.2	13.2	36.3
950	C 62	191.5	182.7	12.1	33.9
950	C 63	193.4	183.7	12.1	34.3
+165°F Testing Temperatures					
1100	C 71	144.0	131.3	15.0	43.9
1100	C 72	144.6	132.9	14.3	44.5
1000	C 68	164.3	152.6	12.9	40.0
950	C 64	179.3	166.6	10.7	35.7
950	C 65	180.3	165.9	10.7	34.3

Table 6

CRACK ARREST FRACTURE TOUGHNESS OF 4140 STEEL
CCA Specimens, W = 2.25 inch, B_N/B = 75, T-L Direction

½-inch thick

Spec. No.	Yield Strength ksi	Test Temp. °F	a_o in.	a_f in.	K_o ksi-in$^{\frac{1}{2}}$	K_f ksi-in$^{\frac{1}{2}}$
C 15	160	RT	0.802	1.570	131.2	75.3
C 16	160	RT	0.789	1.560	149.0	80.8
C 17	150	RT	0.781	1.567	157.1	84.2
C 18	150	RT	0.786	1.630	157.6	79.8
C 19	135	RT	0.789	1.407	171.1	107.9
C 20	140	0	0.816	1.084	135.4	124.1
C 26	180	RT	0.805	1.080	86.2	80.0
C 30	160	0	0.815	1.228	111.1	87.6
C 36	180	165	0.772	1.764	139.6	61.3
C 37	180	-65	0.775	1.632	89.2	46.8
C 38	180	250	0.776	1.621	131.4	67.5
C 40	160	165	0.778	1.730	162.4	73.9
C 41	160	-65	0.795	1.799	120.9	54.1
C 42	160	250	0.775	1.722	160.5	71.2
C 44	140	165	0.779	1.324	197.3	132.6
C 45	140	0	0.000	1.108	0.0	126.1
C 46	140	165	0.775	1.210	167.2	136.1
C 5	200	RT	0.768	1.250	76.7	55.0
C 50	160	330	0.792	1.671	150.9	74.1
C 51	160	-150	0.820	1.567	64.8	44.7
C 52	160	0	0.823	1.264	119.6	91.8
C 7	185	RT	0.762	1.439	106.8	63.5
C 8	185	RT	0.762	1.504	120.9	66.1
C 54	180	0	0.734	1.154	115.5	83.8
C 55	180	75	0.724	1.289	103.7	77.2
C 56	180	0	0.734	1.173	109.8	79.3
C 57	180	150	0.733	1.251	107.6	75.1
C 60	140	-65	0.732	1.060	162.7	139.6
3/4 inch thick						
B 5	210	RT	0.780	1.379	77.7	50.8
B 6	210	RT	0.762	1.304	75.9	52.5
B 8	190	RT	0.772	1.277	97.7	70.0
B 15	160	RT	0.786	1.444	134.9	84.0
B 16	160	RT	0.784	1.442	131.3	81.6
B 17	155	RT	0.787	1.475	153.6	91.1
B 18	155	RT	0.785	1.523	151.6	86.0
B 19	140	RT	0.790	1.243	182.0	137.9
B 20	140	RT	0.785	1.323	164.4	116.4

Materials
Research
Laboratory
Inc

Table 7

CRACK ARREST FRACTURE TOUGHNESS OF 1340 STEEL
($\frac{1}{2}$ inch thick)
CCA specimens, W = 2.25 inch, B_N/B = .75, T-L Direction

Spec. No.	Yield Strength ksi	Test Temp. °F	a_o in.	a_f in.	K_o ksi-in$^{\frac{1}{2}}$	K_f ksi-in$^{\frac{1}{2}}$
D 1	135	RT	0.786	1.666	144.9	72.0
D 2	135	RT	0.787	1.652	131.5	65.8
D 22	180	RT	0.774	1.427	80.3	51.3
D 31	140	RT	0.750	1.573	143.5	74.5
D 32	140	RT	0.750	1.580	133.3	68.3
D 33	140	-65	0.769	1.519	101.9	63.0
D 34	140	-65	0.774	1.404	100.4	64.9
D 35	160	RT	0.766	1.461	80.8	48.1
D 36	160	RT	0.775	1.315	88.6	60.4
D 37	160	-65	0.775	1.632	89.2	46.8
D 38	160	-65	0.772	1.601	86.0	46.5
D 45	180	165	0.766	1.341	84.7	55.8
D 46	180	165	0.761	1.306	89.5	62.7
D 47	160	165	0.763	1.485	89.9	54.8
D 48	160	165	0.762	1.372	84.4	55.7
D 49	140	165	0.759	1.369	110.5	71.9
D 50	140	165	0.760	1.270	98.5	71.6
D 51	180	-65	0.792	1.005	46.8	45.9
D 52	180	-150	0.797	1.199	41.2	37.4
D 53	180	75	0.793	1.247	67.7	52.4
D 54	180	0	0.798	1.272	59.2	44.8
D 55	160	250	0.798	1.781	123.4	56.6
D 56	160	330	0.794	1.808	117.7	51.5

B

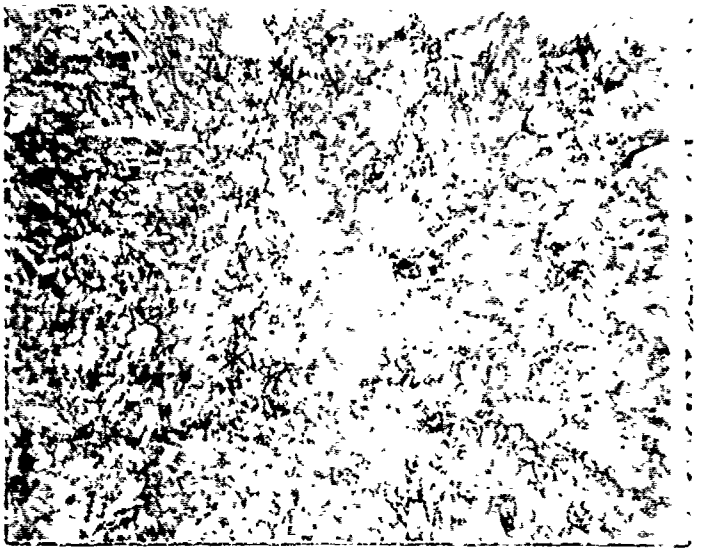

C

D

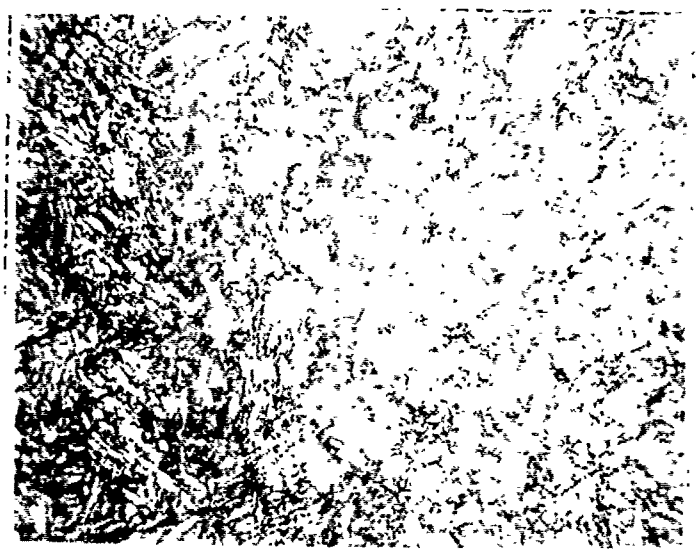

Fig. 1 Microstructure of heats B (4140 - 3/4 inch thick), C (4140 - ½ inch thick) and D (1340 - ½ inch thick) after normalize, quench and temper. (1500X, nital etch.)

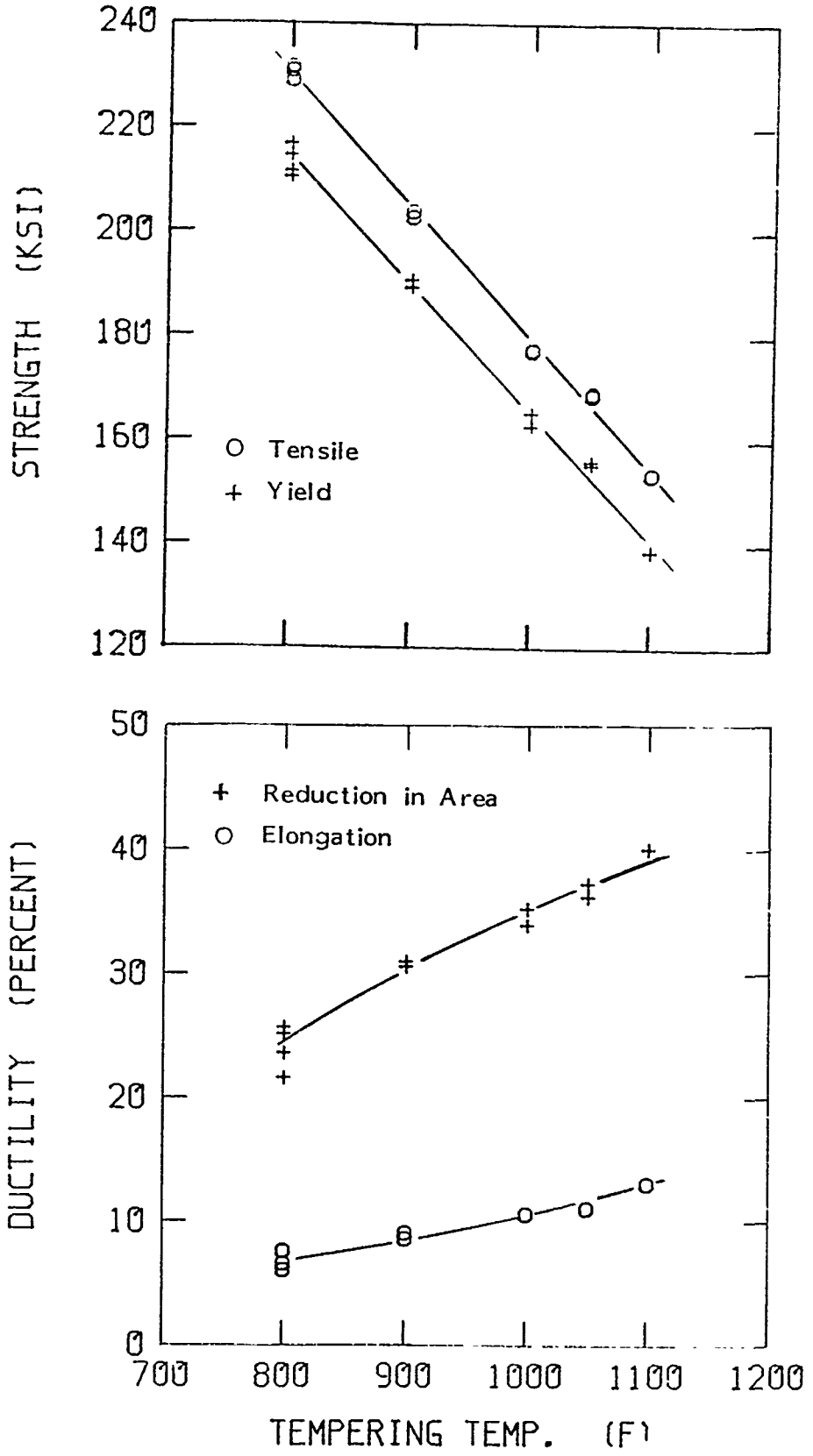

Fig. 2 Tensile properties of 3/4 inch thick 4140 steel (B plate) at room temperature as a function of tempering temperature.

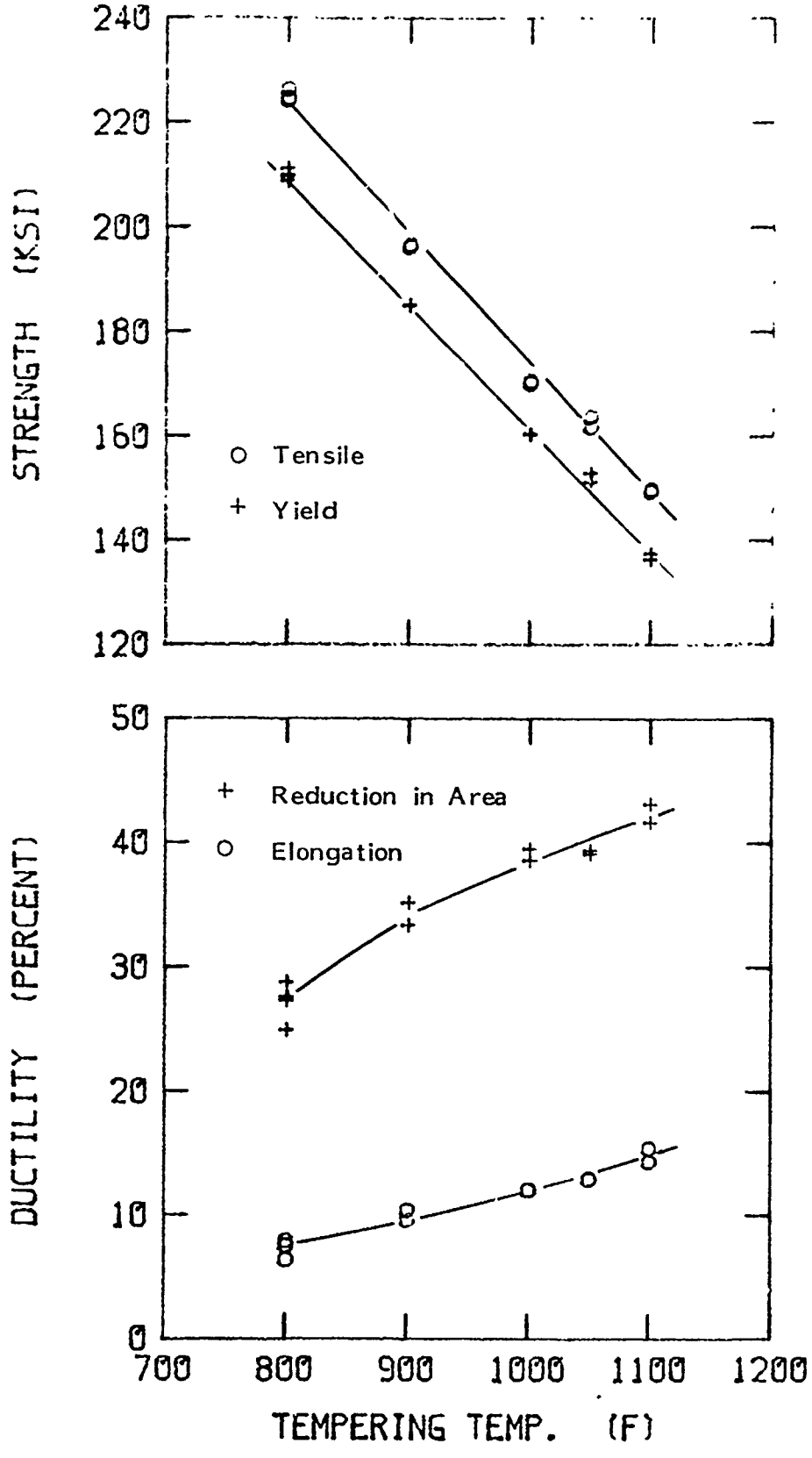

Fig. 3 Tensile properties of ½ inch thick 4140 steel (plate C) at room temperature as a function of tempering temperature.

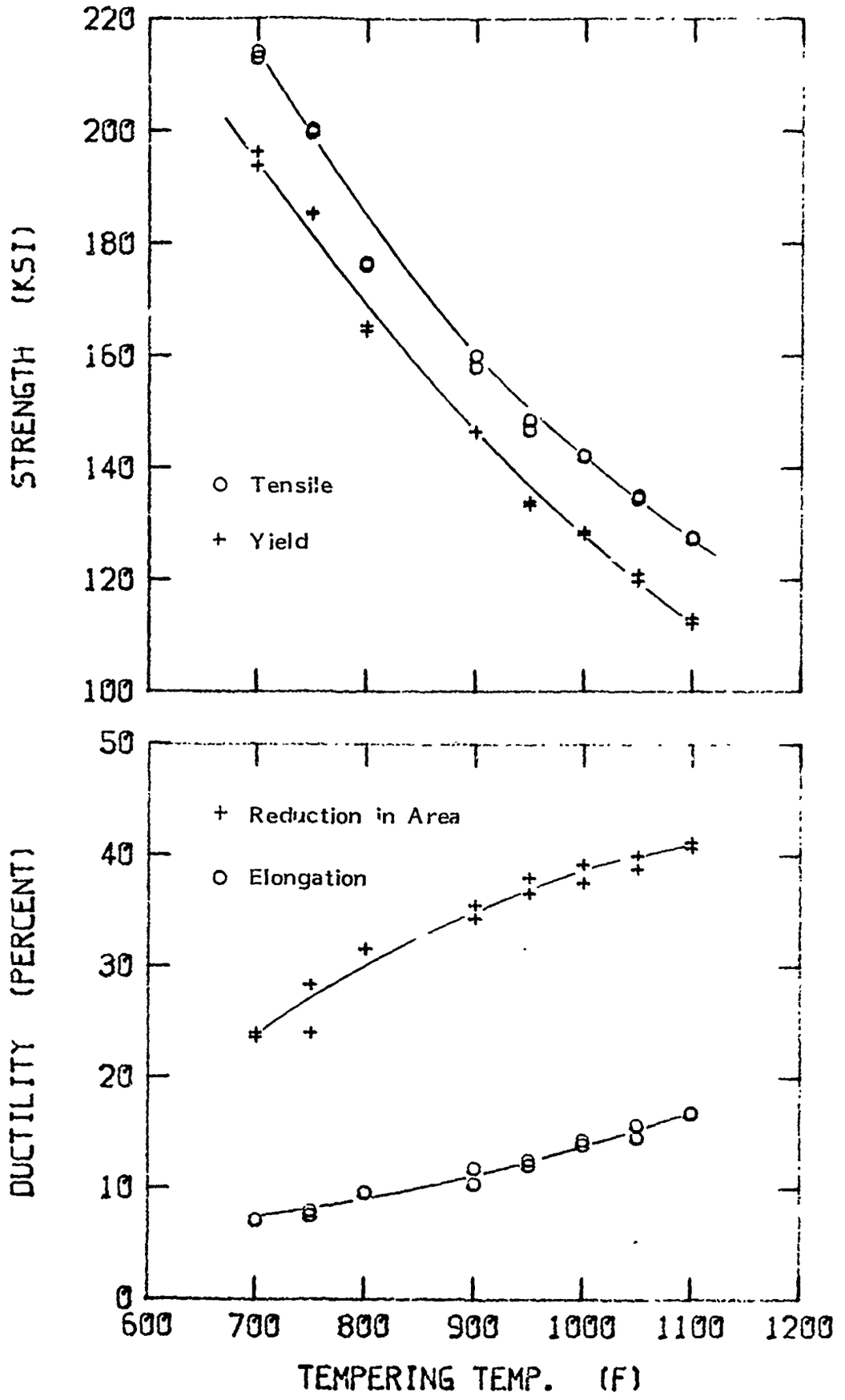

Fig. 4 Tensile properties of ½ inch thick 1340 steel (plate D) at room temperature as a function of tempering temperature.

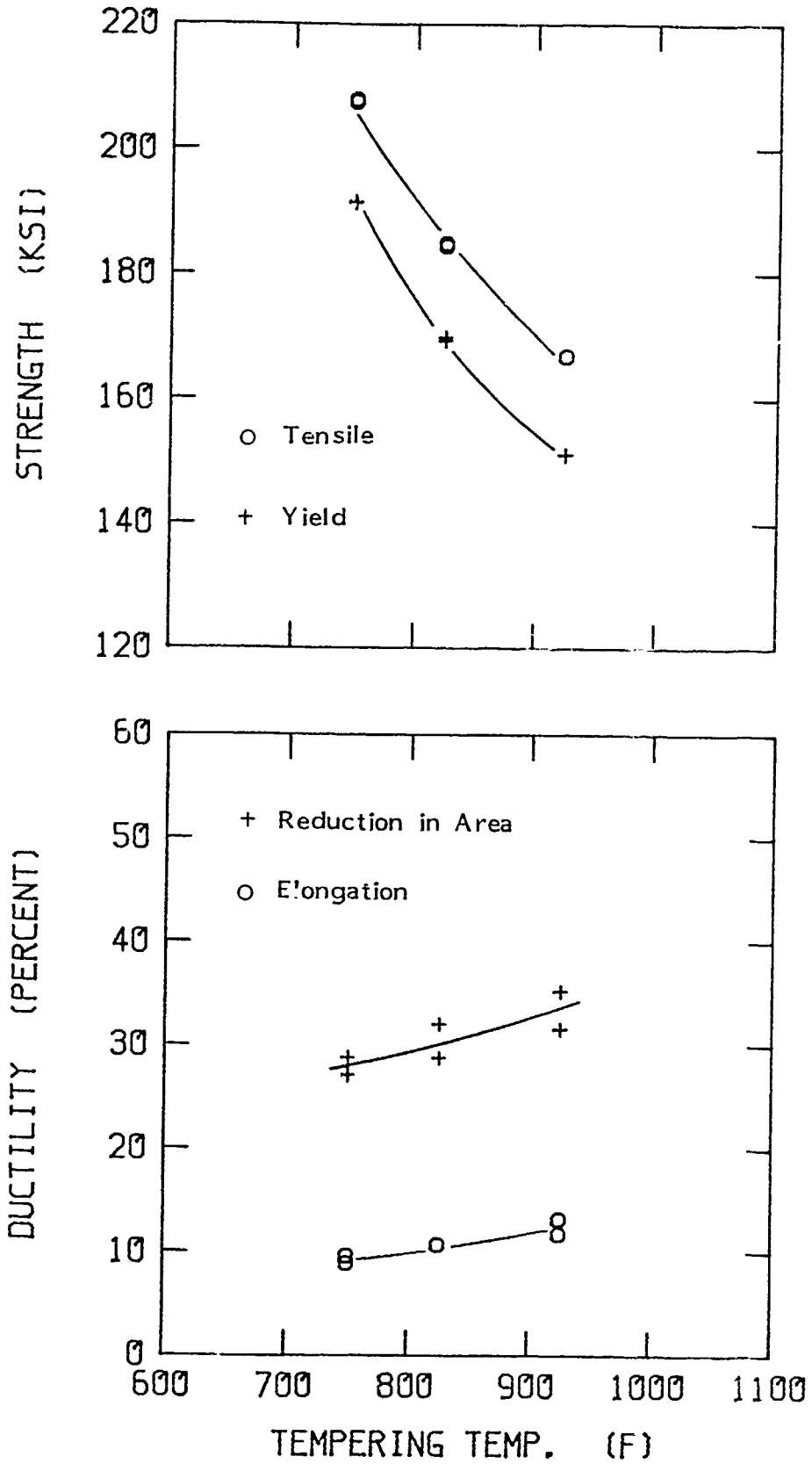

Fig. 5 Tensile properties of ½ inch thick 1340 steel (plate D) at -65F as a function of tempering temperature.

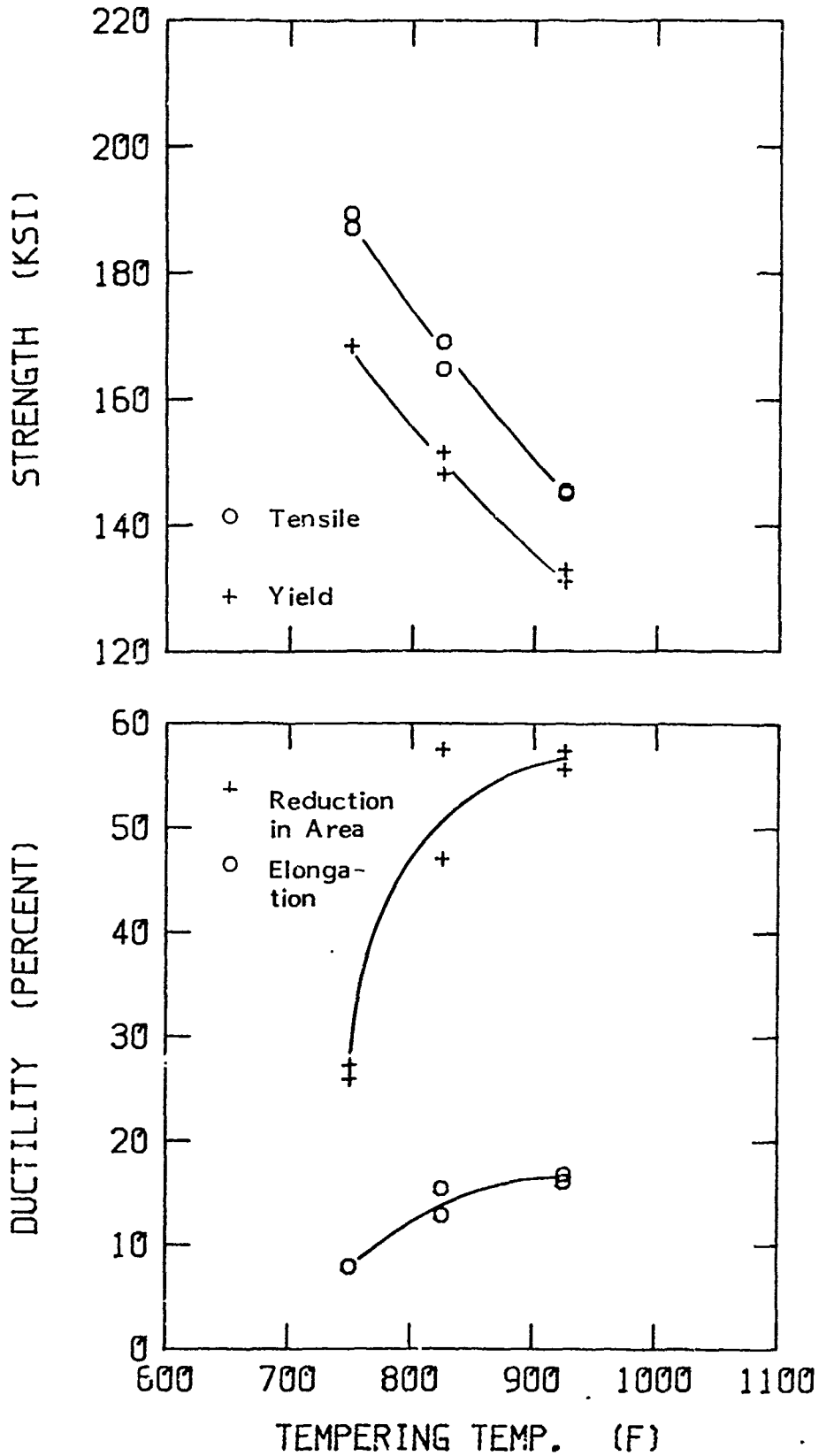

Fig. 6 Tensile properties of ½ inch thick 1340 steel (plate D) at 165°F as a function of tempering temperature.

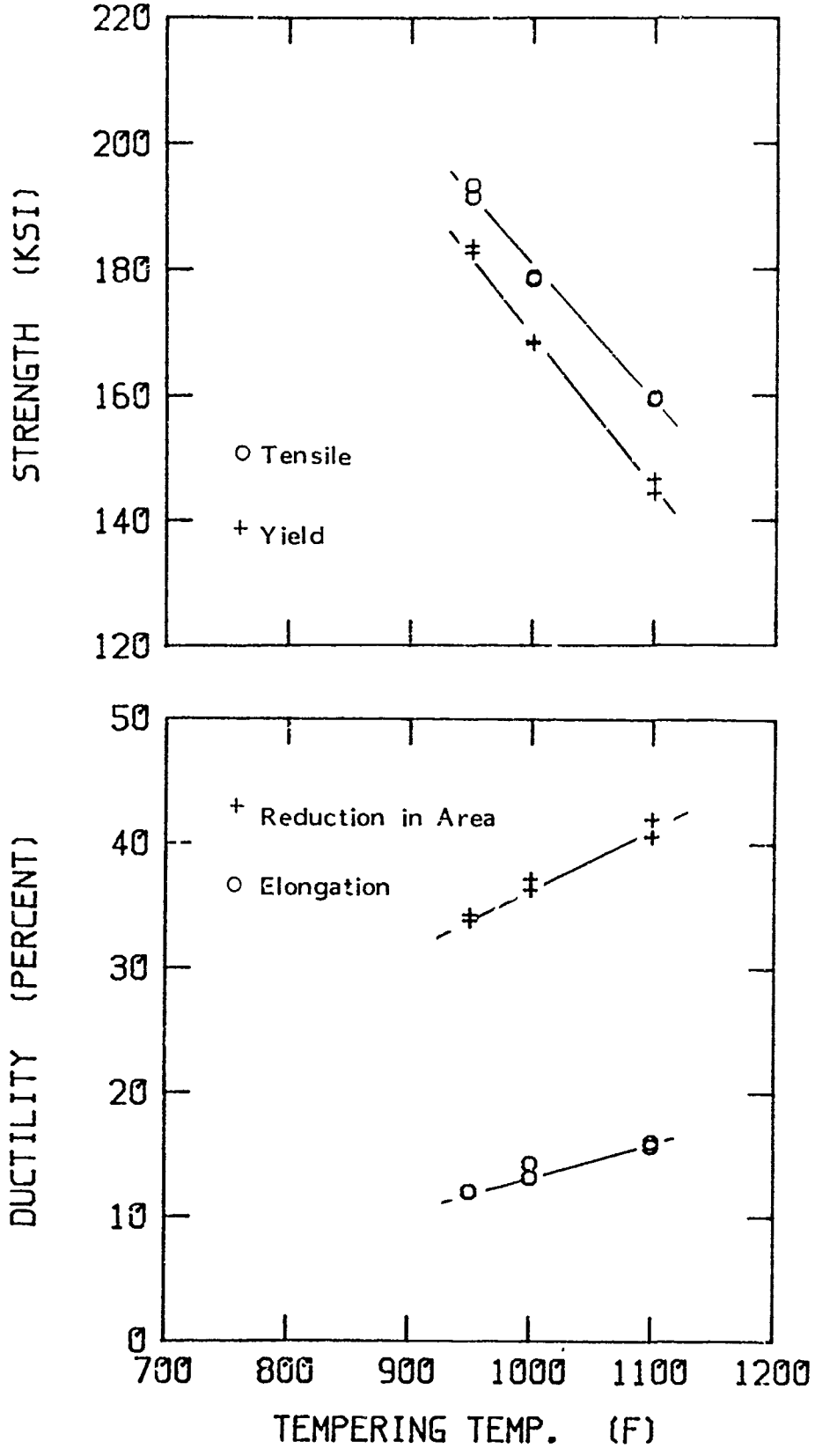

Fig. 7 Tensile properties of ½ inch thick 4140 steel (plate C) at -65°F as a function of tempering temperature.

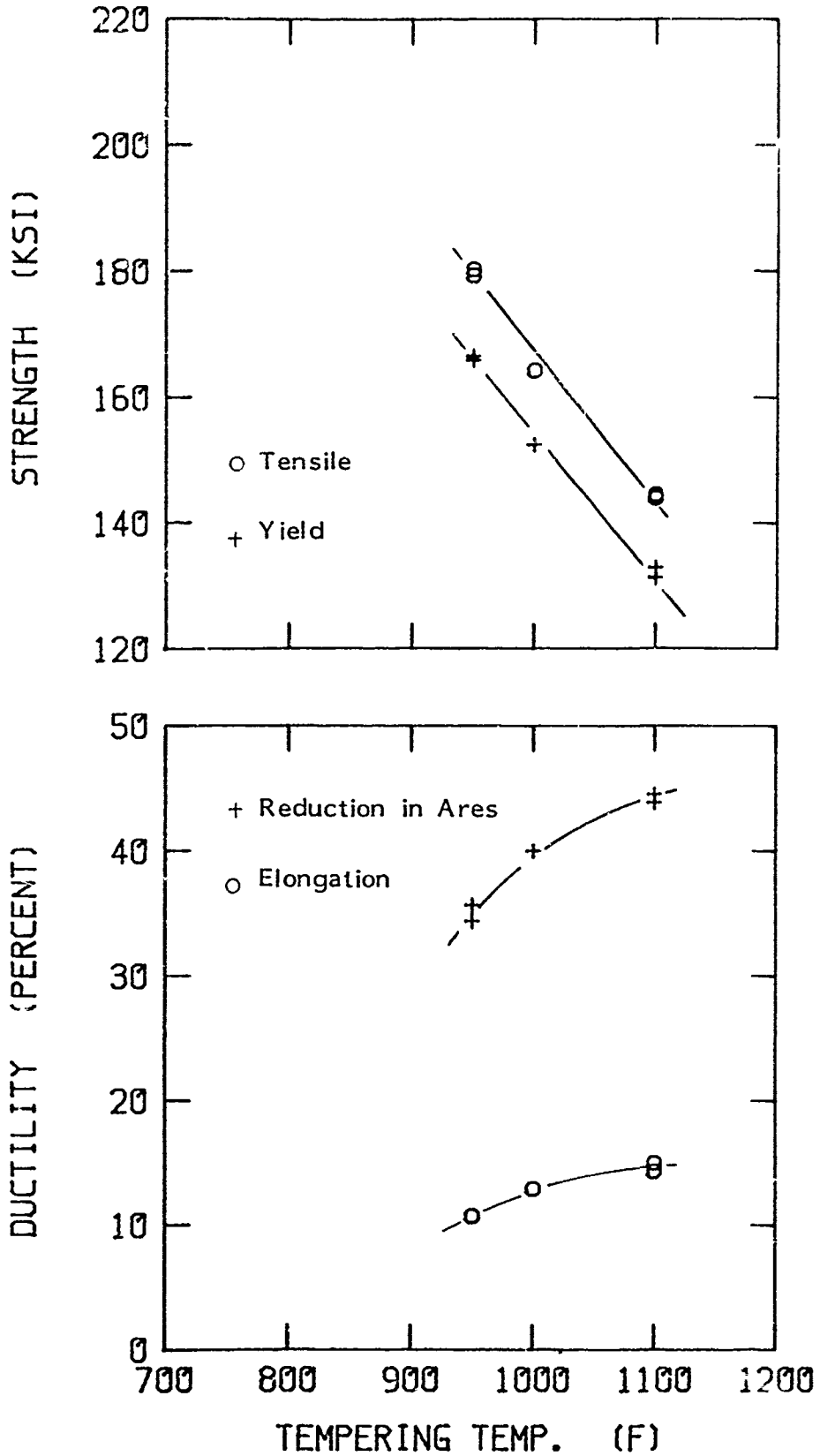

Fig. 8 Tensile properties of ½ inch thick 4140 steel (plate C) at 165°F as a function of tempering temperature.

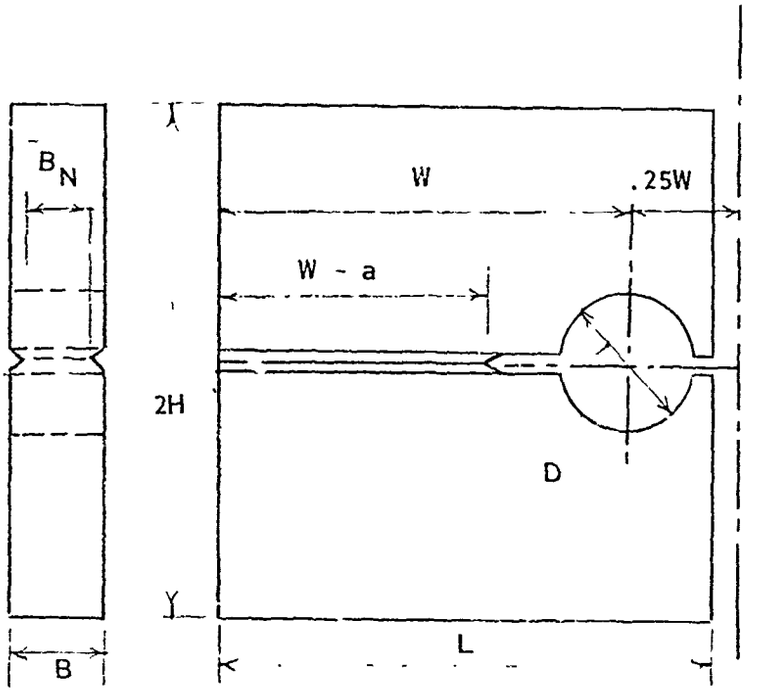

Knife edge

W	=	2.250
W - a	=	1.463
D	=	0.750 + 0.005 - 0.000
2H	=	2.700
L	=	2.700
B_N/B	=	0.75
t	=	0.113

(All dimensions inches)

Fig. 9 Dimensions of compact crack arrest (CCA) test specimen.

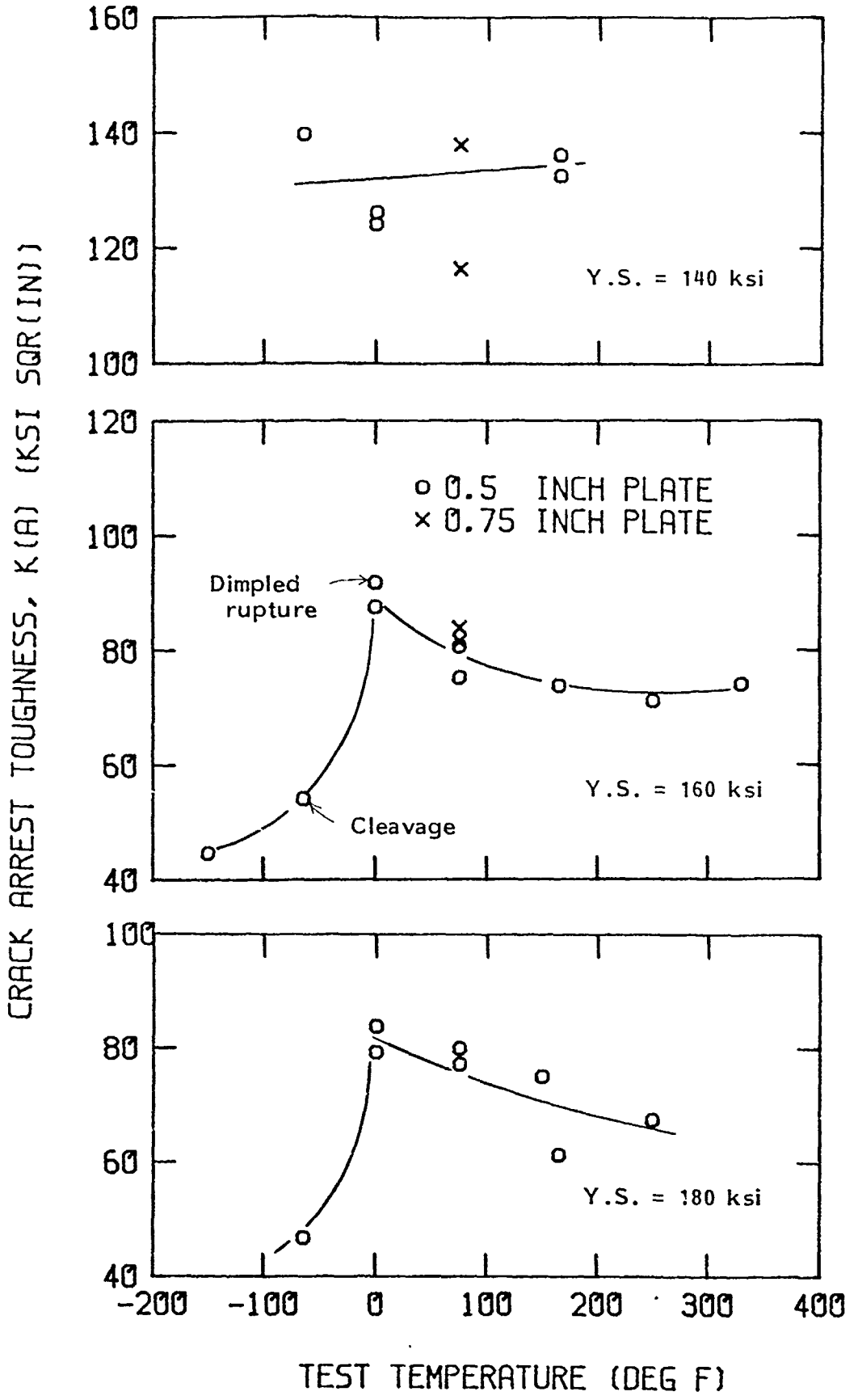

Fig. 10 Crack arrest fracture toughness of 4140 steel as a function of test temperature (0.05 and 0.75 inch thick plate).

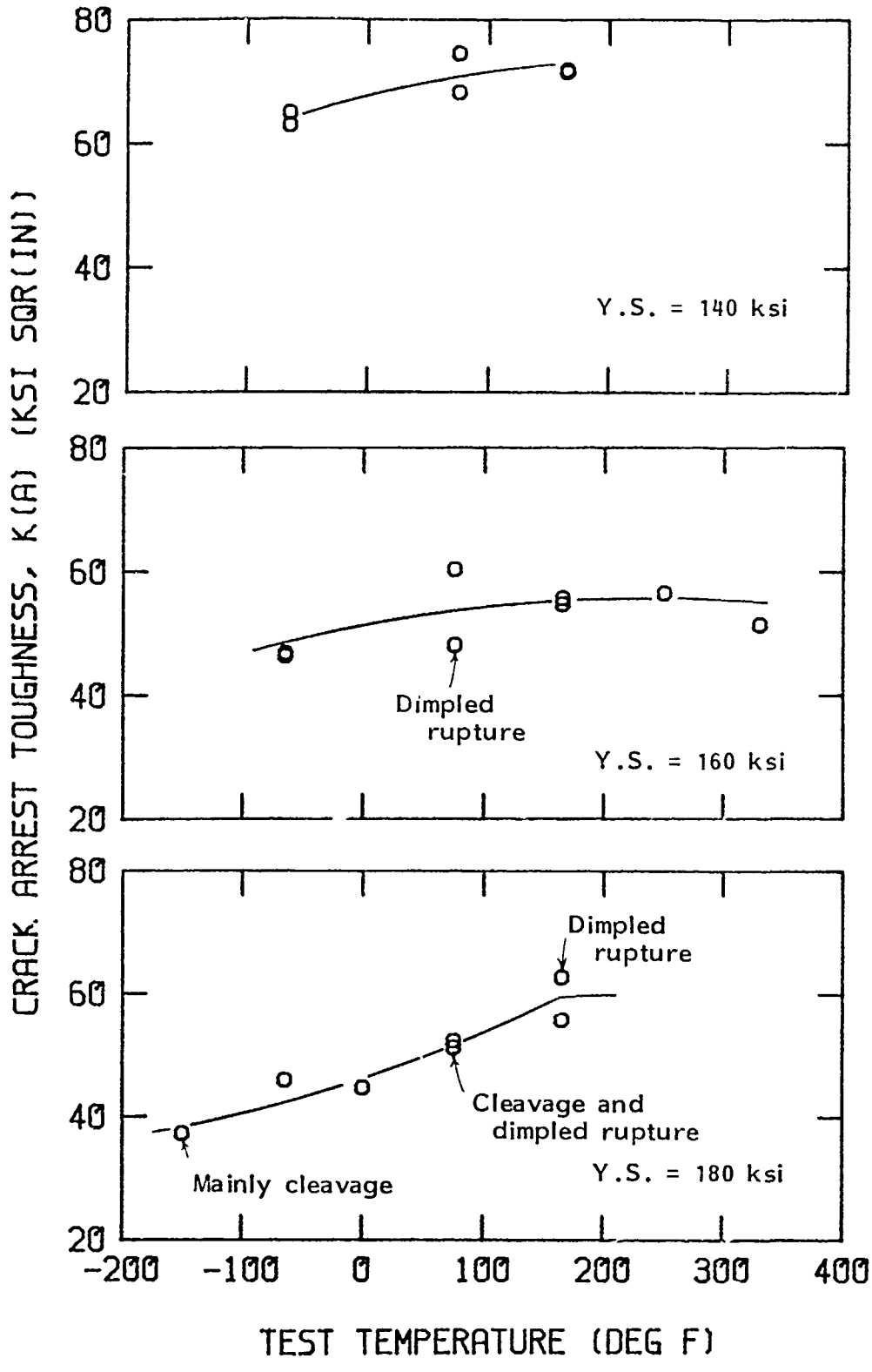

Fig. 11 Crack arrest fracture toughness of 1340 steel as a function of test temperature (0.5 inch thick plate).

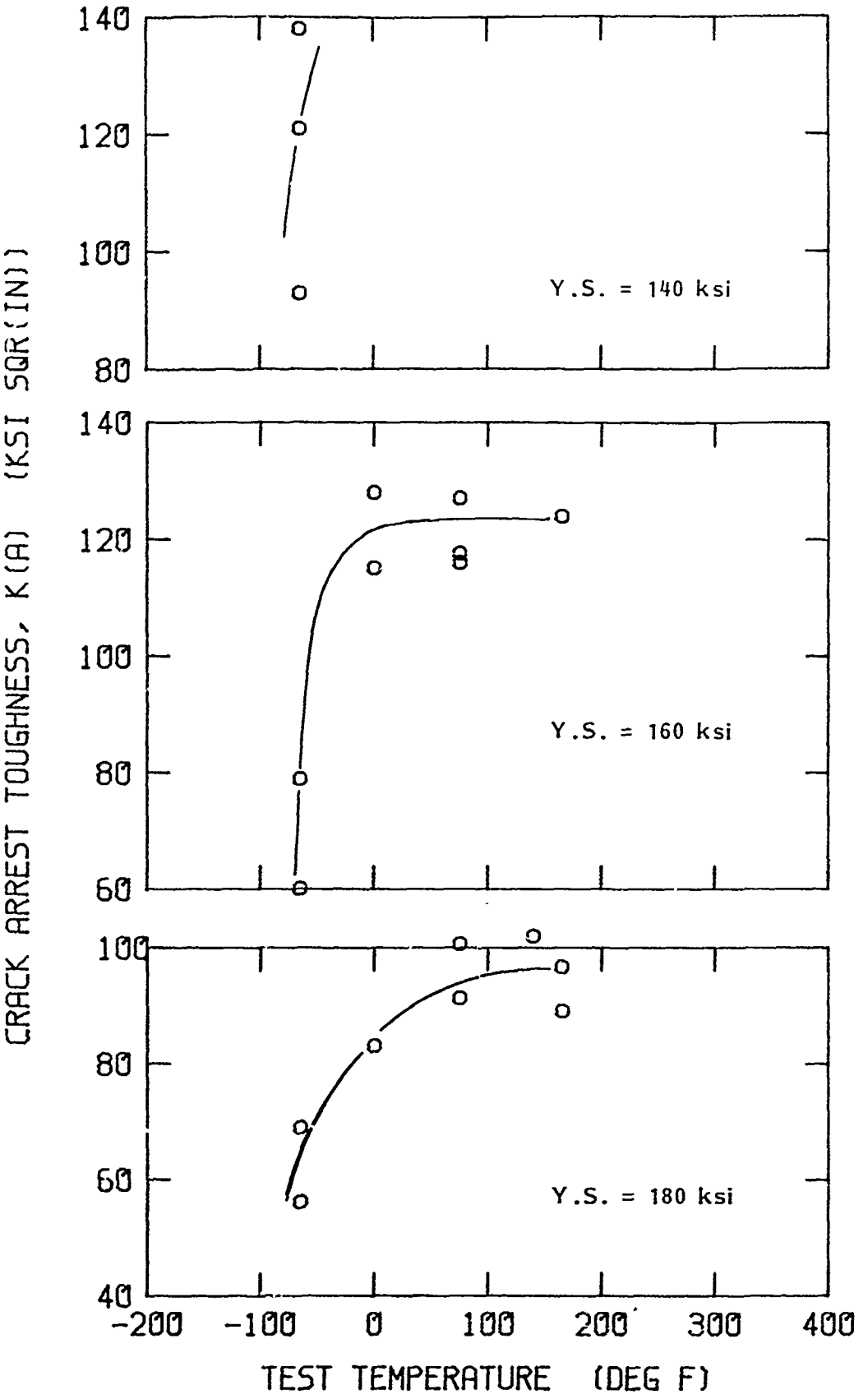

Fig. 12 Crack arrest fracture toughness of 4340 steel as a function of test temperature (1 inch thick plate)[1].

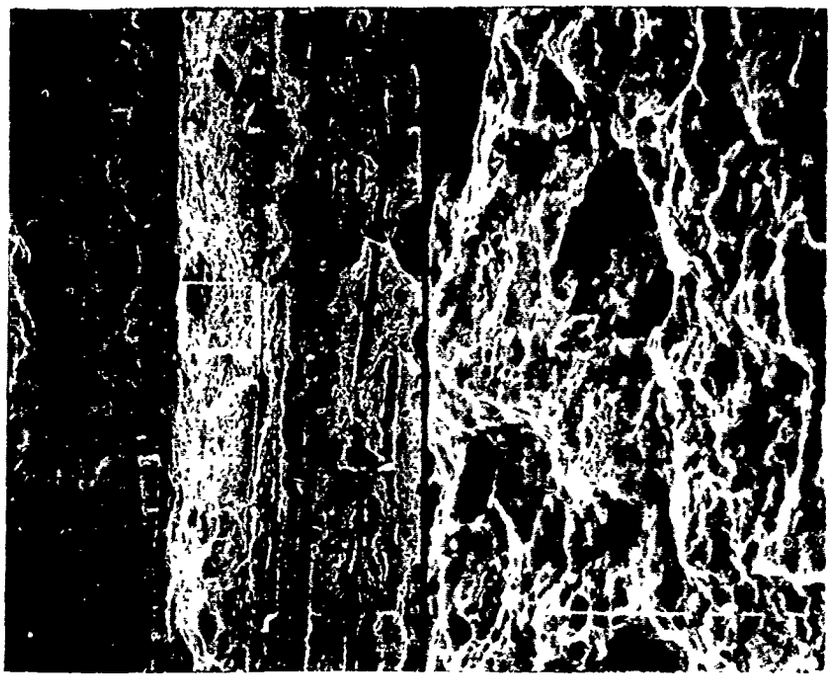

200X 2000X

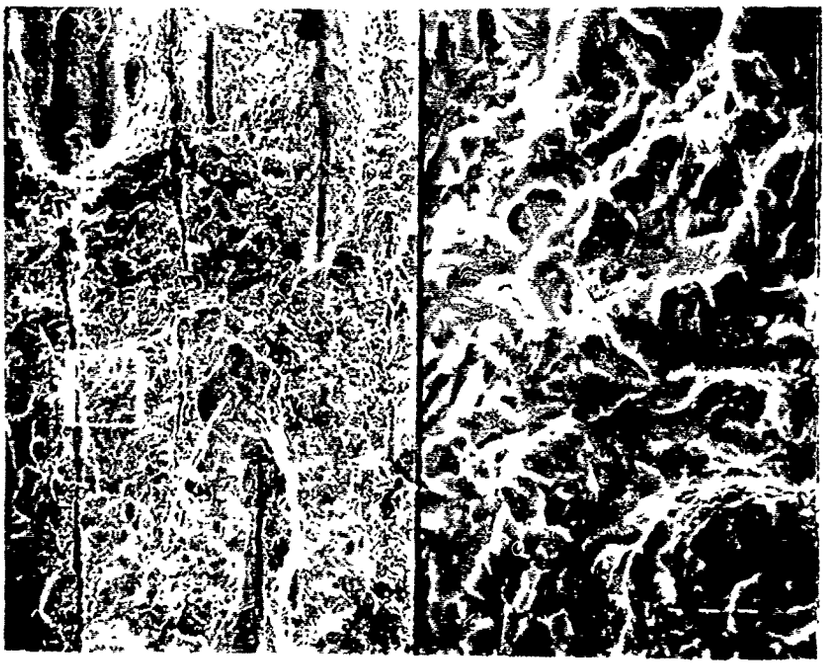

200X 2000X

Fig. 13 Fracture appearance of 4140 steel (160 ksi yield strength) Top: Test at 0°F; Bottom: Test at -65°F.

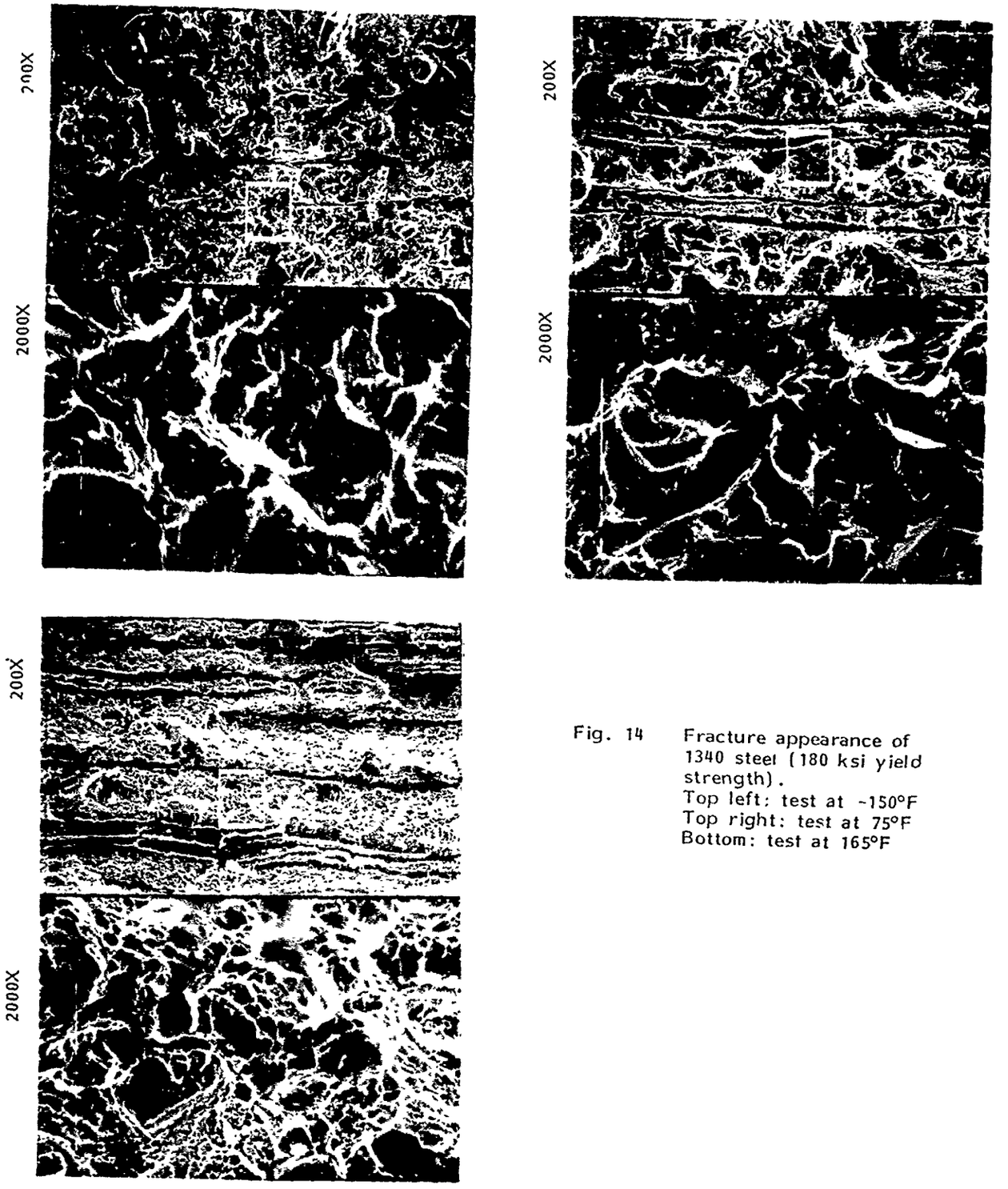

Fig. 14 Fracture appearance of 1340 steel (180 ksi yield strength).
Top left: test at -150°F
Top right: test at 75°F
Bottom: test at 165°F

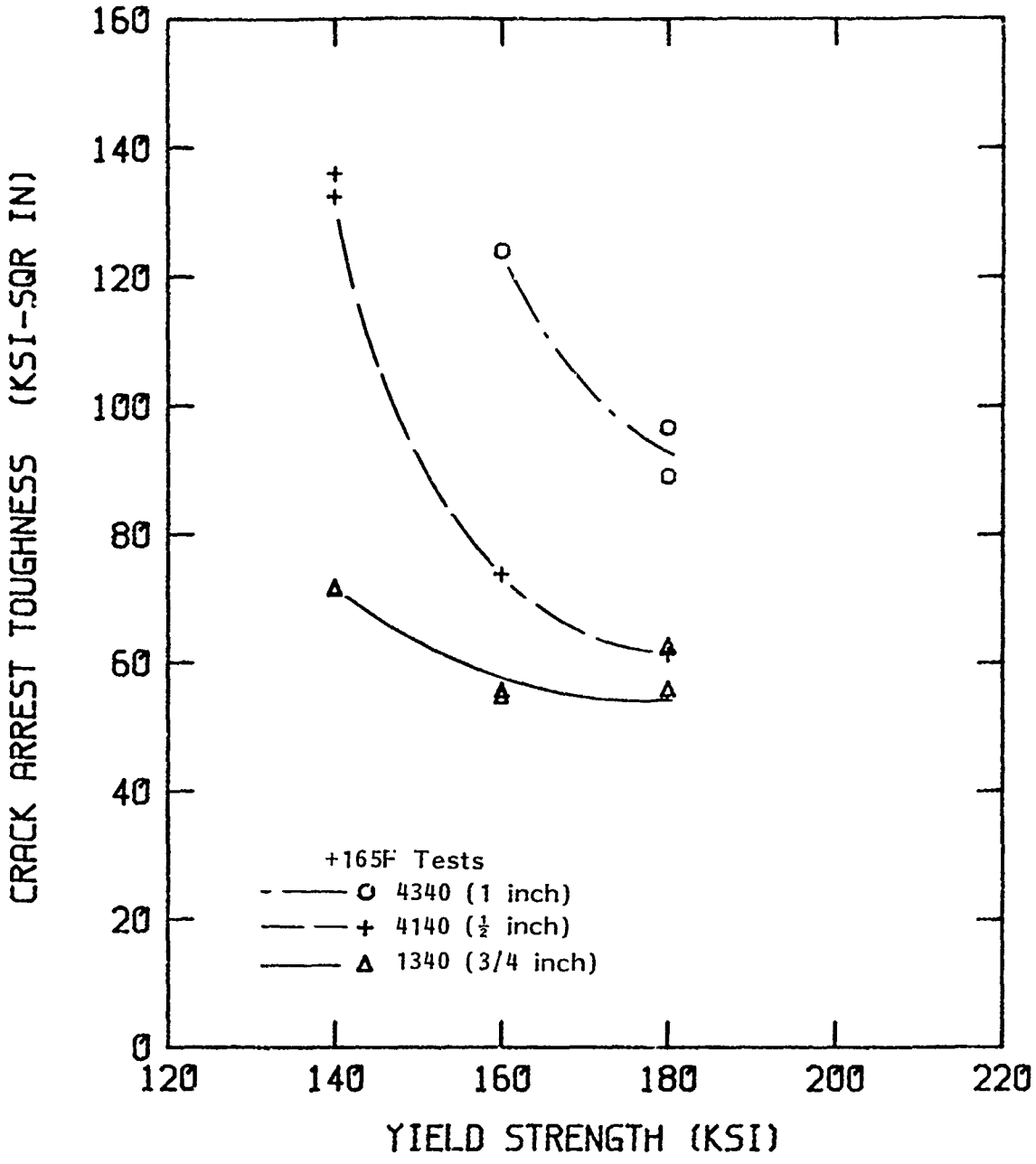

Fig. 15 Comparison of the crack arrest toughness of the three steels when tested at +165°F.

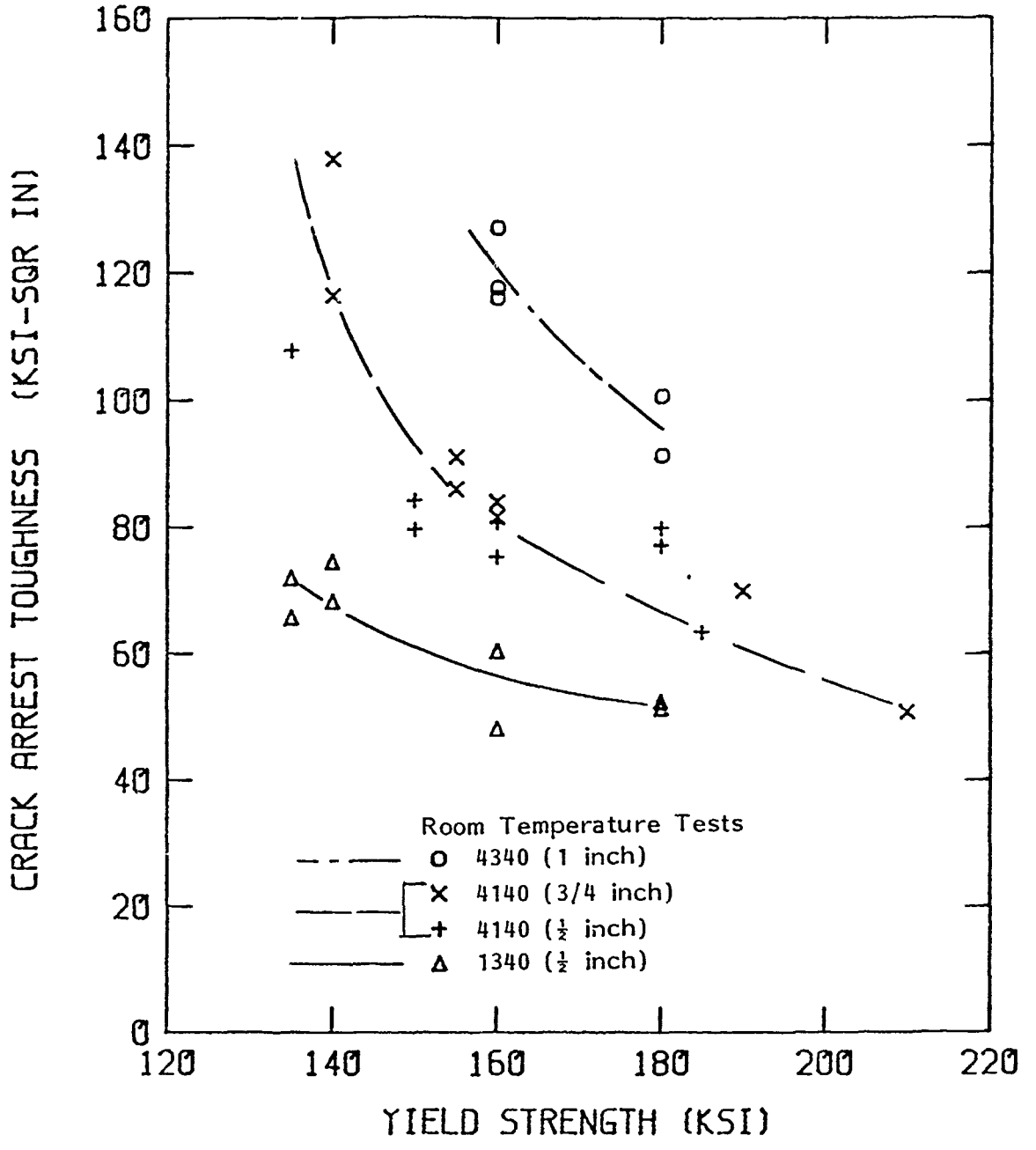

Fig. 16 Comparison of the crack arrest toughness of the three steels when tested at room temperature.

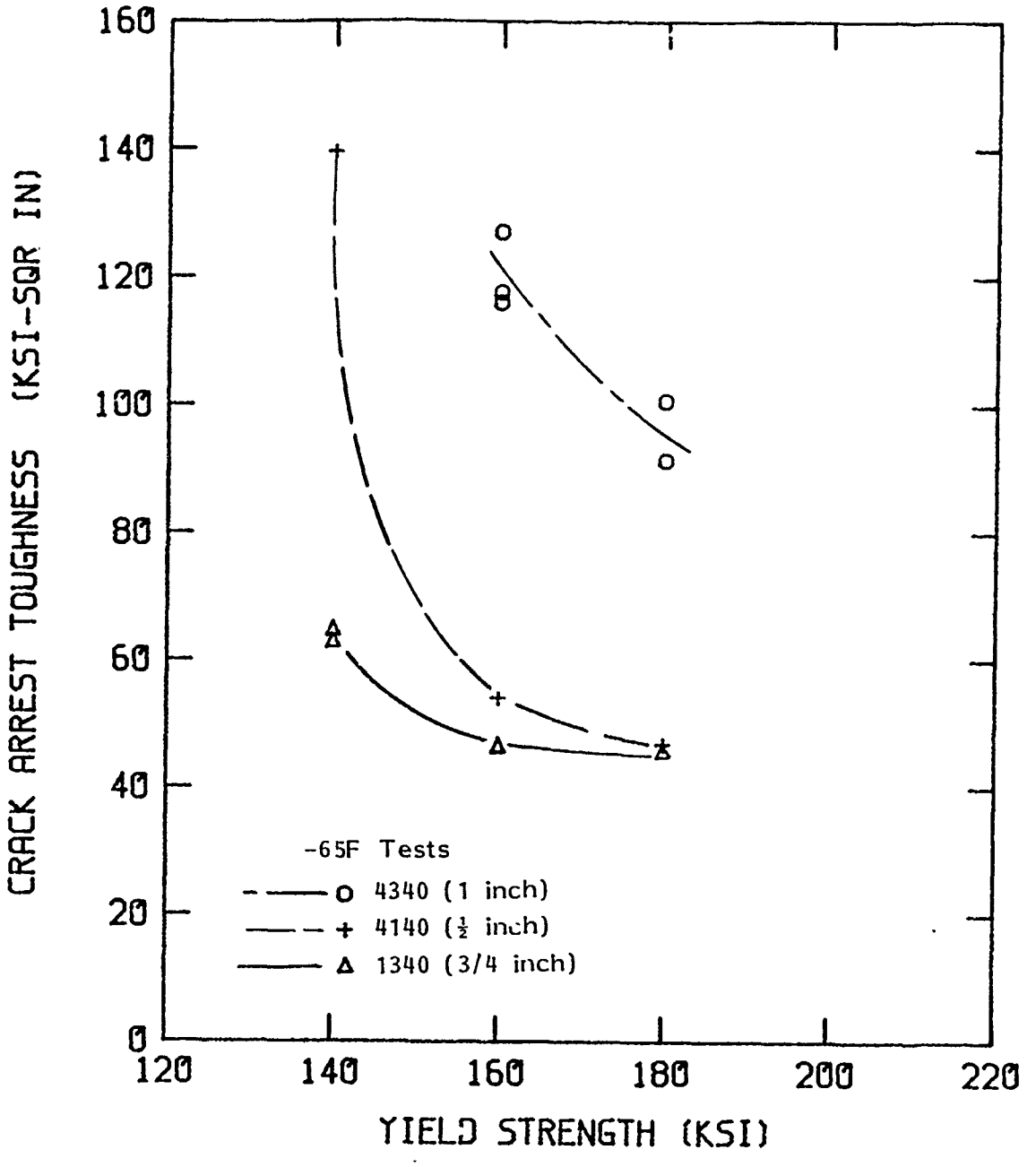

Fig. 17 Comparison of the crack arrest toughness of the three steels when tested at -65°F.

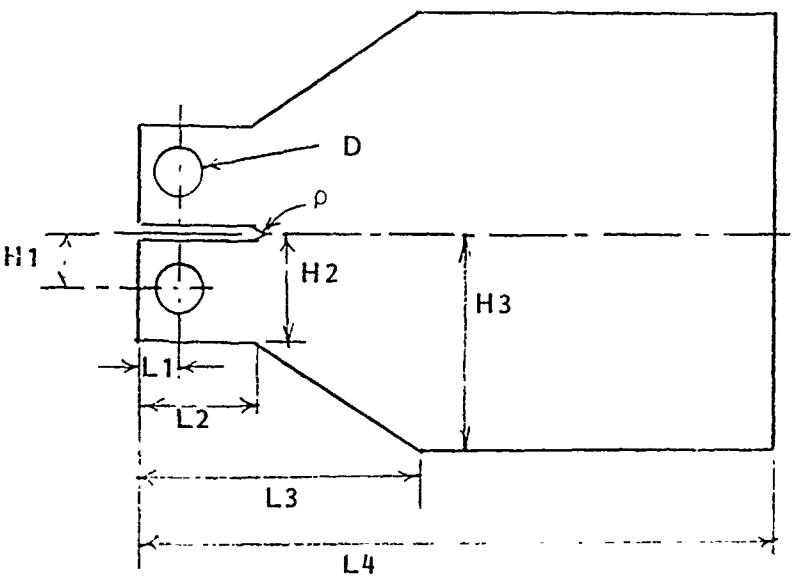

D = 0.500 + 0.005 - 0.000

H1 = 0.5 H2 = 1.00 H3 = 2.00

L1 = 0.42 L2 = 1.04 L3 = 2.70 L4 = 6.00

(All dimensions, inches)

Fig. 18 Dimensions of tapered double cantilever beam (TDCB) specimen.

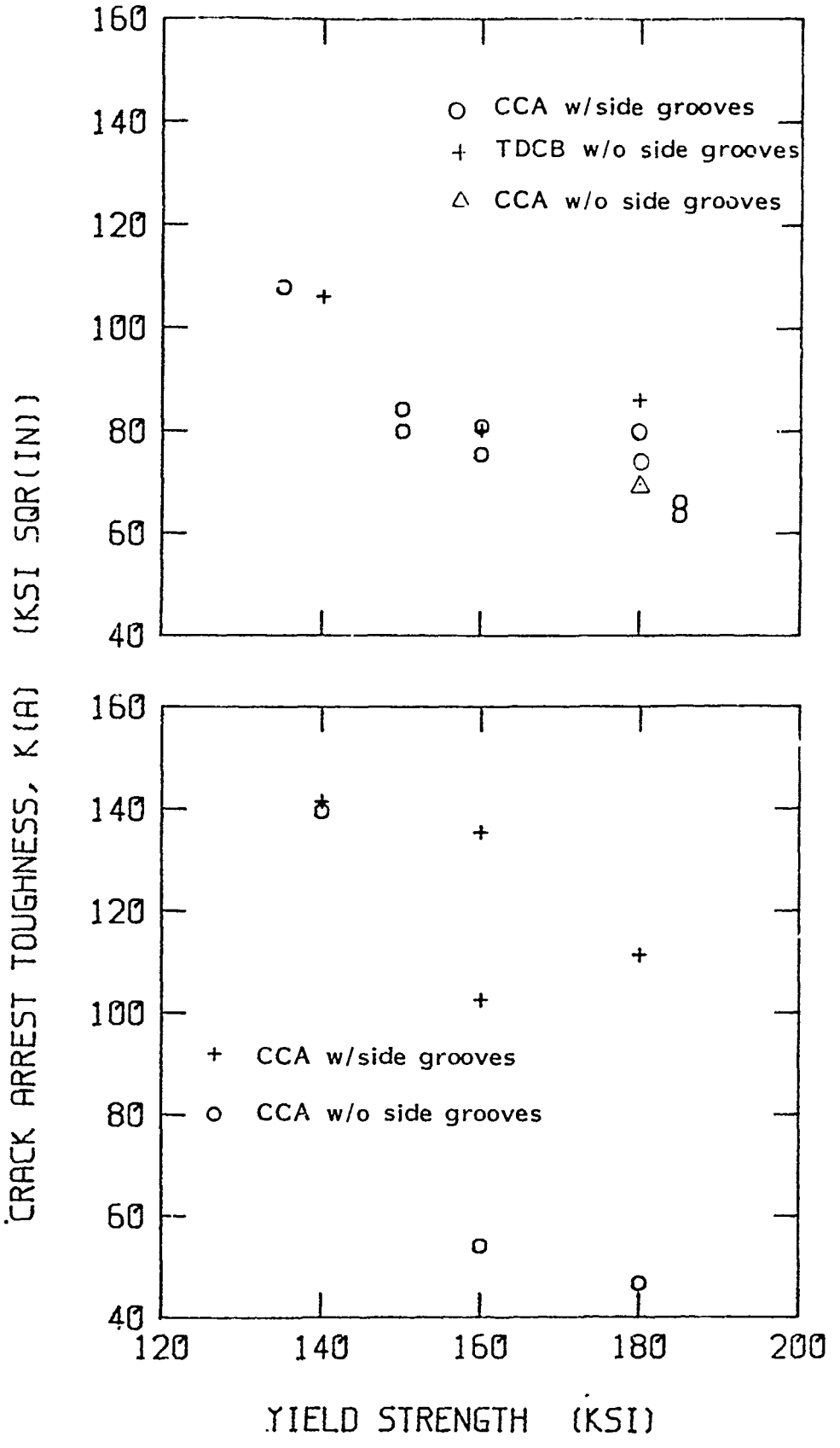

Fig. 19 Comparison of K_a with and without side grooves.
Top: room temperature tests.
Bottom: -65 tests.

References

1. E. J. Ripling, J. H. Mulherin and P. B. Crosley, "Crack Arrest Toughness of Two High Strength Steels (AISI 4140 and AISI 4340). To be published in AST Met. Trans.

2. P. P. Milella, C. W. Marschall and A. R. Rosenfield, "A Method to Obtain Crack-Opening Force in Transverse-Wedge Loading," to be published.

7.0 Appendix (Non-Optical Methods for Measuring Crack Lengths)

If unside-grooved CCA specimens are to be used for measuring K_a, some method is needed to define the length of tunneled cracks. The most promising method for doing this is to make a measurement from which an "effective crack length" can be implied. Two techniques were evaluated for measuring effective crack length: one, a double displacement method, and the other, a technique suggested by Milella for calculating wedge friction, from which the opening load can be calculated.

7.1 Double Displacement Method

In order to evaluate the double displacement method, the specimen was modified by adding two holes at -0.3W, i.e., in the direction away from the specimen mouth, as shown in Fig. A-1. Two aluminum specimens of this type were prepared, one with side grooves, and the other without. The specimens were incrementally saw cut along their centerplane, and the ratio of the displacements at -0.3W (V_1) to mouth opening displacement -0.25W, (V_o) was measured as a function of saw cut length (a/W). A plot of these data are shown in Fig. A-2. The data from the two specimens combined gave a standard error in a/W of 0.0240 when the data were represented by a second order polynomial. For an arrested crack length of a/W - 0.6, this standard error in crack length produced an error in K_a of about five percent.

In a second test series, the two displacements V_1 and V_o were measured on the specimens used to evaluate K_a by the standard method. For these tests, the crack lengths at initiation (a_o) and arrest (a_f) were measured at the completion of the test. The accuracy of the relationship between the ratio V_1/V_o and a_o and a_f was then determined by comparing the second order polynomial fit developed in Fig. A-2 with these measured crack lengths, Fig. A-3. In spite of the fact that almost all of the measured crack lengths lie above the curve, a double displacement technique might be an adequate method for measuring effective crack lengths.

7.2 Milella Method for Calculating Wedge Friction and, Hence, Compliance[2].

In the absence of friction a plot of wedging force versus wedge travel would follow the same line when the wedge is extracted as when it is pushed into the specimen. When the wedging force is opposed by friction, however, there are separate curves for pushing and for extracting the wedge, as shown in Fig A-4 (a). As proposed by Milella, this behavior can be analyzed to calculate the coefficient of friction between the wedge and the split pins. Referring to the force diagrams in Fig. A-4b, it can be seen that the difference between the "pushing" and "extracting" curves in Fig. A-4a is a simple consequence of the change in the direction of the friction forces. A force balance can be made to obtain an expression for the coefficient of friction, μ. This gives

$$\mu = A - (A^2 - 1)^{\frac{1}{2}} \qquad (A-1)$$

where

$$A = \left(\frac{F_1 + F_2}{F_1 - F_2}\right) \frac{1}{\sin 2\alpha}$$

and where α is the wedge half-angle and F_1 and F_2 are the forces indicated in Fig. A-4 (a). For pushing the wedge, the specimen opening load, P, is related to the wedging force, F, by the equation

$$P = \tfrac{1}{2} F \frac{1 - \mu \tan \alpha}{\tan \alpha + \mu} \qquad (A-2)$$

In the present work the friction analysis was used to calculate crack length. The calculation is based on the fact that there is a unique value of the ratio, V_o/P, at a given crack length; or equivalently given a value of V_o/P, the crack length can be inferred. Values of the coefficient of friction were obtained through eq. (A-1) from loading-unloading sequences carried out before and after the test;

that is, with the machine notched uncracked specimen and with the specimen containing the arrested crack. Measurement of the wedging load and opening displacement at the crack initiation point and at the crack arrest point were used with eq. (A-2) to determine the ratio of V_o/P corresponding respectively to the original machined notch length and the arrested crack length. Earlier measurements of V_o/P as a function of a/W could then be consulted to calculate values of a/W* from the test-derived values of V_o/P.

The results obtained are plotted in Fig. A-5. The initial slot lengths were all close to a/W = 0.35, but the values inferred from the friction analysis centered about a/W = 0.4, and ranged nearly from 0.35 to 0.45. This difference probably results from the fact that there is some plastic flow developed at the crack tip when the wedge is cycled. For the arrested cracks the friction analysis estimated a/W values that were lower than the actual measured ones. Unfortunately, the friction forces were not evaluated for the saw-cut specimens so that the amount of error attributed to the physical crack length measurements cannot be obtained.

---

* For calculational purposes, the experimental results relating a/W and V_o/P were fitted with the following mathematical expression:

$$a/W = 0.218226 + 6.50462\,x - 28.5645\,x^2 + 54.6405\,x^3 - 43.7041\,x^4 + 14.712\,x^5$$

where

$$x = EBV_o/P$$

7.3 Conclusions

The test results discussed above suggest that the double displacement technique, at least, has promise for evaluating effective crack length. Unfortunately, the Milella method was not used on the saw-cut specimens, so that this method was not adequately evaluated.

When either method, double displacement, or friction was used to evaluate effective crack length, the implied value of $\underline{a}$ was always shorter than the directly measured one (see Figs. A-3 and A-5). This suggests that the method now used for measuring arrested crack lengths should be re-examined.

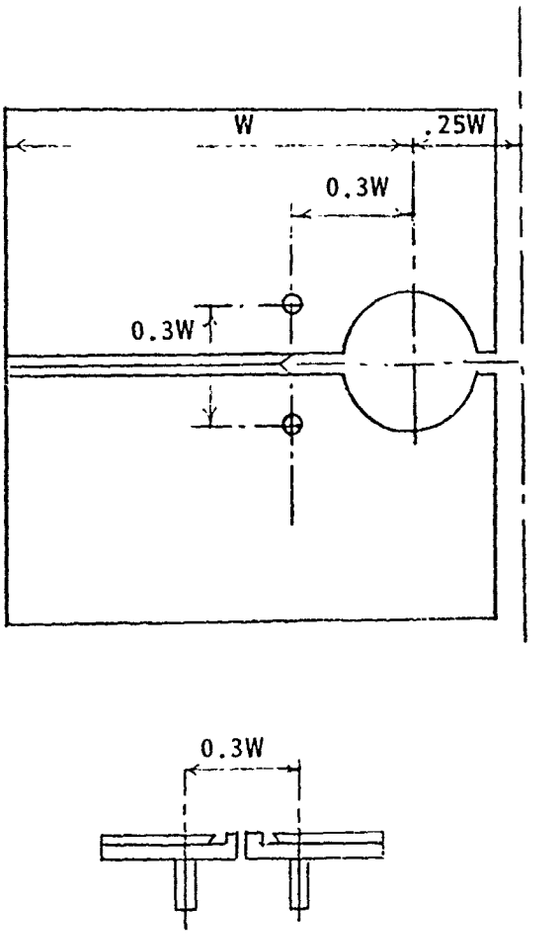

Knife edges for measuring displacement at 0.3W

Fig. A-1 Specimen modification and knife edges for measuring displacement at 0.3W.

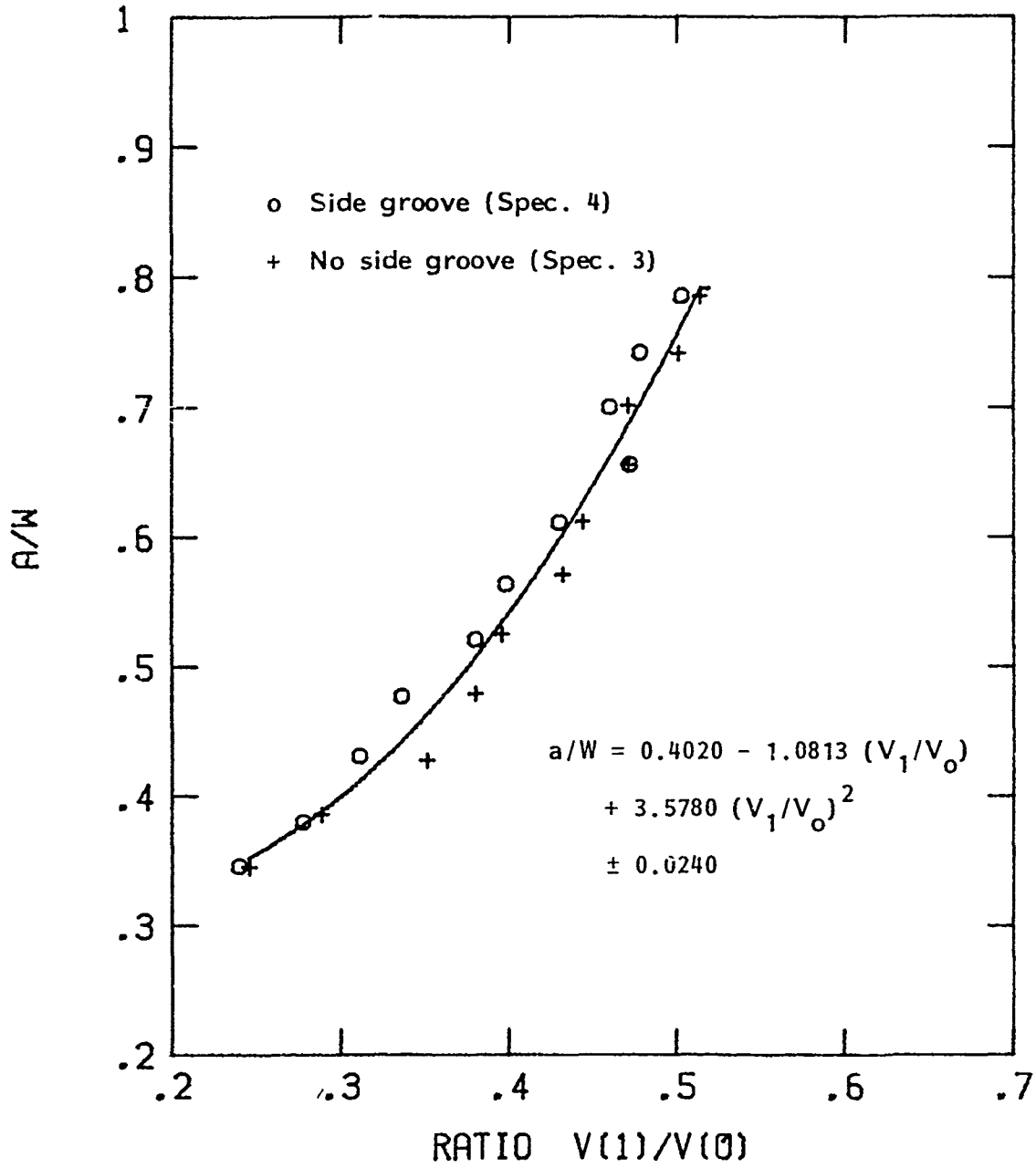

Fig. A-2 Sawed-crack length as a function of the displacement ratio V_1/V_o (V_1 at -0.3W; V_o at + 0.25W).

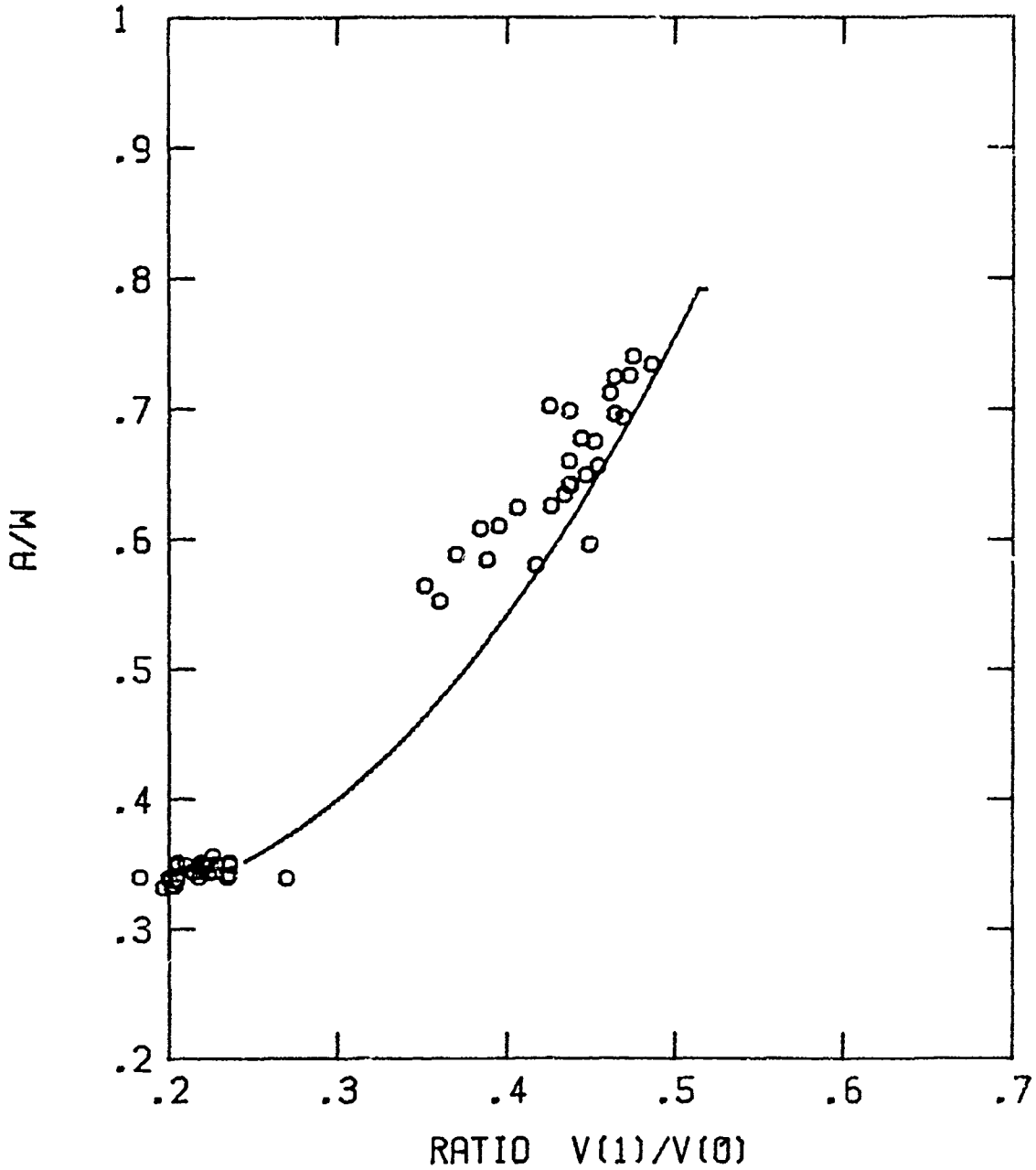

Fig. A-3 Comparison of actual values of a/W with curve developed in Fig. 2 using double displacement.

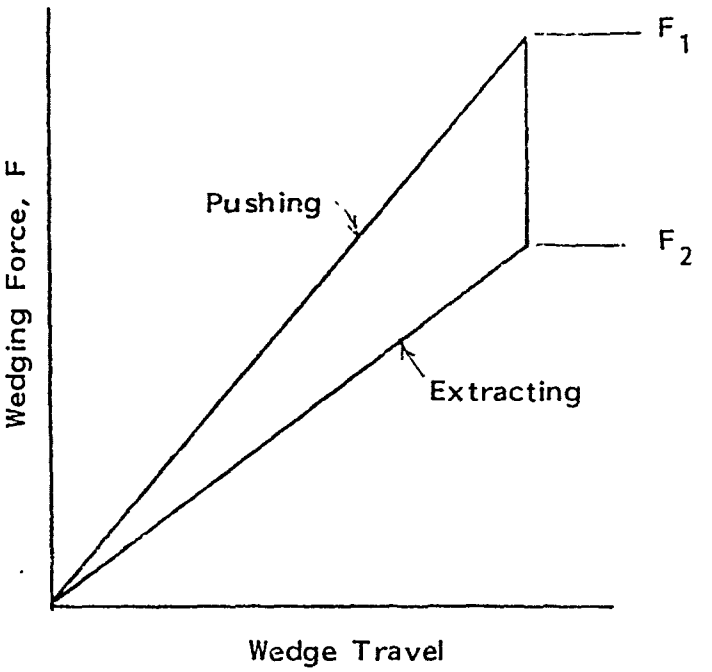

(a) Wedging force versus wedge motion on pushing and extracting the wedge in the presence of friction.

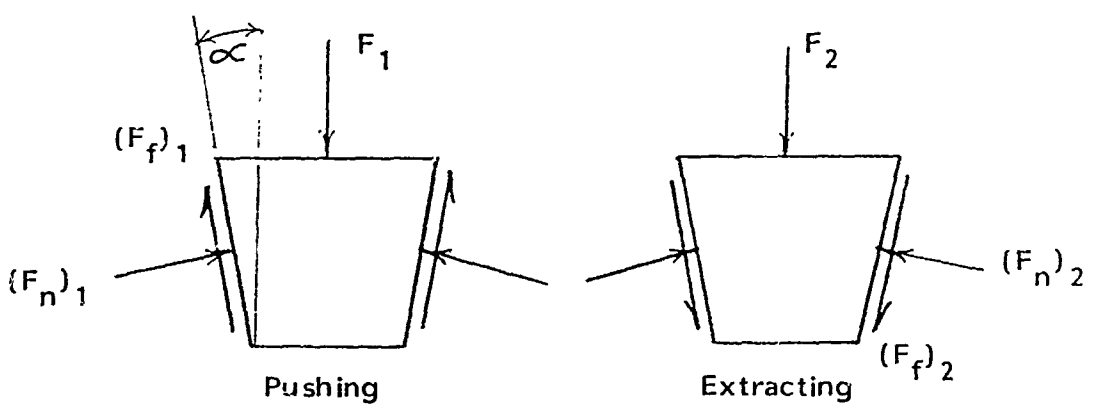

(b) Force diagrams for pushing and extracting wedge.

Fig. A-4 Analysis of friction forces in wedging.

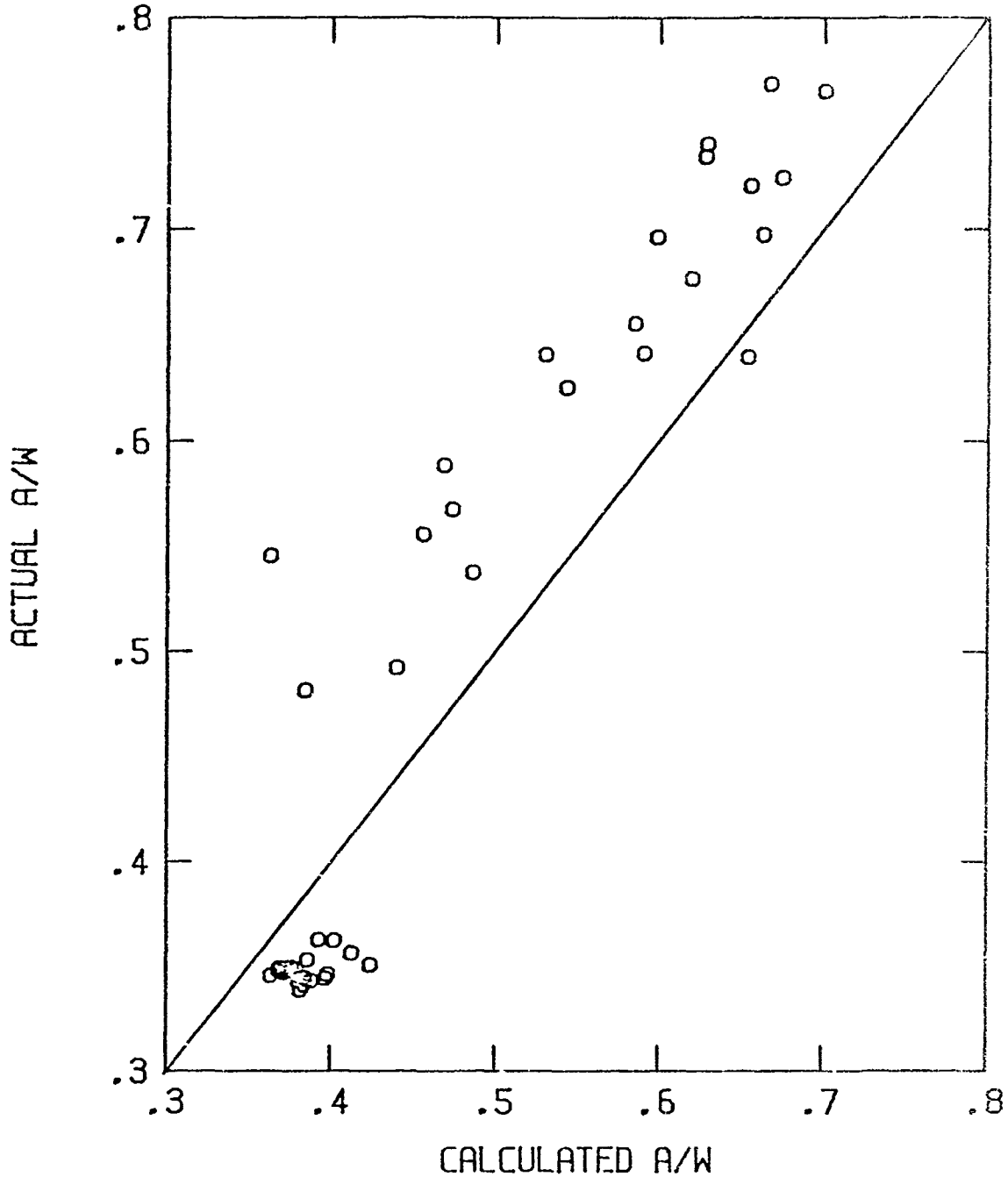

Fig. A-5 Comparison of actual and calculated crack lengths using the Milella friction calculation.

END

DATE
FILMED

7-83

DTIC